NAVWEPS REPORT 8525
NOTS TP 3580
COPY 57

PENDULUM-TYPE NUTATION DAMPER USED IN THE NASA ATMOSPHERIC STRUCTURE SATELLITE, S-6

by

H. L. Newkirk
Aeromechanics Division
Weapons Development Department

27060

ABSTRACT. A reliable passive device was developed for quickly damping out nutational motion of the spin-stabilized NASA S-6 satellite (Explorer 17). A list of the Bureau of Naval Weapons drawings for it is given. The operating principles for this twin-pendulum damper were determined with the aid of a small table-top gyroscopic model. Final developmental testing was done with a full-scale dynamical simulator.

Formulas for each of the three basic design criteria are derived. These formulas are (1) for tuning the damper to the nutational disturbance, (2) for the selection of the viscous friction coefficient of the pendulum hinge, and (3) for the guarantee that the desired final balanced and stable configuration of damper and satellite will be obtained.

Author

U.S. NAVAL ORDNANCE TEST STATION

China Lake, California

June 1965

U. S. NAVAL ORDNANCE TEST STATION

AN ACTIVITY OF THE BUREAU OF NAVAL WEAPONS

J. I. HARDY, CAPT., USN
Commander

WM. B. MCLEAN, PH.D.
Technical Director

FOREWORD

As a part of research studies in exterior ballistics under the Bureau of Naval Weapons Task Assignment RMMO-42-008/216-1/F008-09-001, theoretical and experimental work was carried out at the Naval Ordnance Test Station (NOTS) during 1959 on the problem of nutation damping and undamping in rotating bodies. Possible application of this work to a satellite being planned by the National Aeronautics and Space Administration (NASA) was suggested by Mr. J. D. Nicoliades of the Bureau of Naval Weapons, RT-1.

Subsequent discussion between NASA and NOTS personnel led to further study directed specifically toward the NASA satellite nutation damper. Because the study results continued to be promising, development and fabrication of full-scale devices were undertaken and completed at this Station. The project objective was to develop, design, and fabricate a nutation damper for the NASA Atmospheric Structure Satellite, S-6 (Explorer 17), and this report documents the work that accomplished that objective. The effort described was performed during the period from March 1960 to March 1963, and the work carried out for NASA was supported by funds transferred to this Station under NASA Purchase Order S-4562-G.

This report was reviewed for technical adequacy by W. R. Haseltine, Research Department; G. E. Sutton, University of Nevada; and D. F. Fitzpatrick, the NASA Project Coordinator for this project.

Released by
F. H. KNEMEYER, Head,
Weapons Development Department
31 March 1965

Under authority of
Wm. B. McLEAN
Technical Director

NOTS Technical Publication 3520
NAVWEPS Report 8525

Published by ..... Weapons Development Department
Manuscript 40/MS 64-22
Collation ..... Cover, 40 leaves, abstract cards
First printing ..... 135 numbered copies
Security classification ..... UNCLASSIFIED

CONTENTS

NOTATION

A Polar moment of inertia of the main body; a coefficient in an expression for the pendulum swinging in gravity (Appendix A); also the area of the surfaces causing viscous friction (Appendix B)

B Transverse moment of inertia of the main body; also a coefficient in an expression for the pendulum swinging in gravity (Appendix A)

C Maximum amplitude of the pendulum swinging in gravity (Appendix A)

F Viscous friction-force (Appendix B); also force on the pendulum bob in the centrifugal field (Appendix C)

H_o Total angular momentum vector of the simulator (Fig. 31)

I Moment of inertia of a pendulum about the hinge axis

K A non-dimensional design parameter (hinge-friction coefficient) from Ref. 4

L Length of a damper pendulum from the hinge axis to the c. g.

M Mass of the main body

R Inner radius of cylindrical container used in viscosity measurement

S Non-dimensional stability parameter

T Kinetic energy

V Relative velocity of the surfaces in viscosity determination (Appendix B)

a Radial distance to a pendulum hinge-pin

b Real radical in the solution for the pendulum swinging in gravity (Appendix A)

c Restoring moment coefficient for a pendulum swinging in gravity (Appendix A)

d Separation of the surfaces (Appendix B); instantaneous distance from the axis of the simulator, or main body, to the total spin axis at the height, h, above the c. g. (Appendix C); also the small displacement error between the center of the nutation damper and the symmetry axis of the main body

g Acceleration of gravity of the earth

h Height from the c. g. of the main body to the plane of operation of the pendulum dampers (Fig. 13)

i The imaginary, $\sqrt{-1}$

k Pendulum-hinge coefficient of friction in "torque = $-k\dot{\varphi}$"

l Length of the shorter cylinder in the pendulum hinge

m Mass of a damper pendulum

n Number of swings of a pendulum (Appendix A)

r Vector positions of the damper masses in the inertial coordinates (Ref. 4); and mean radius of inner and outer cylindrical surfaces (Appendix B)

s Number of turns of the main body, or simulator, from an arbitrary zero

t Time

Δ Orientation angle in the measurement of transverse moment of inertia (Fig. 26)

Θ_R Angle of dynamic unbalance between the symmetry axis and the axis of maximum moment of inertia

Θ_u Dynamic unbalance

Φ Phase angle in an expression for the pendulum swinging in gravity (Appendix A)

Ω In general, spin, or oscillation frequency expressed in radians per second

α Damping coefficient; also a construction angle (Appendix C)

β A non-dimensional design parameter (relative to damper height) from Ref. 4; also frequency (radians per second) of the undamped pendulum in gravity

γ Parameter relating to manufacturing tolerances

δ A non-dimensional design parameter (measure of moment of inertia ratio) (Ref. 4)

η Viscosity of the hinge-damping fluid

θ Instantaneous angle between the axis of the simulator, or main body, and the total angular momentum vector, nutation angle; also the angle of a pendulum swinging in gravity (Appendix A)

λ Coefficient in the exponent in a solution to the pendulum differential equation (Appendix A)

ν Kinematic viscosity

ρ A non-dimensional design parameter (Ref. 4); also the radius of gyration of the pendulum about its c. g. (Appendix A); also the density of the damping fluid

τ Torque arising from hinge friction

φ Displacement angle of a damper pendulum from its desired position

φ_1, φ_2 Two pendulum angles

ω In general, spin, or oscillation frequency expressed in radians per second

ω_N Angular rate of nutation

ω_o Total angular velocity

ω_p Polar component of total angular velocity

ω_T Transverse component of total angular velocity

$\omega_x, \omega_y, \omega_z$ In order, the polar and transverse components of total angular velocity

NASA S-6 Satellite (Explorer 17) and Dynamical Test Vehicle.

INTRODUCTION

In April 1963 from Cape Canaveral, the National Aeronautics and Space Administration(NASA) Atmospheric Structure Satellite, S-6 (Explorer 17) was launched with a Thor-Delta booster and was programmed for a polar orbit of high inclination.[1] The S-6 satellite was designed to measure the composition, density, pressure, and temperature of the rare atmosphere at high altitudes and any variation of these quantities with latitude and time of day. This satellite is spin-stablized with spin axis approximately tangent to the orbit at injection.

In external appearance, the S-6 satellite is a 3-foot-diameter sphere with probes and antennas protruding symmetrically about the polar axis (Fig. 1). The sphere itself consists of a 0.02-inch-thick stainless-steel skin with joints and probe outlets welded except for the joint between the upper and lower parts of the satellite that is closed by 96 bolts and a copper gasket. The air maintained inside of the sphere is at about sea level atmospheric pressure, and because the nature of the experiment is to measure the stated quantities, no leaks through the skin can be tolerated. The general arrangement of components inside the sphere is indicated in Fig. 2. The major part of the total weight (about 370 pounds) consists of the wet-battery power pack, made of Yardney "Silvercels," in various sizes from 2 to 200 ampere-hours. These components of various shapes, sizes, and weights are so arranged that the center of gravity (c. g.) is near the geometrical center of the sphere. Final static- and dynamic-balancing place the c. g. and the greatest principal axis of inertia very close to the symmetry axis about which the sphere rotates in space.

The launching sequence consisted of three stages of boost. The first two stages were guided, or controlled. The last, or injection stage, using an ABL X-248 motor, was spin-stabilized at about 90 rpm (or 1.5 rps). The configuration, with booster attached to the satellite, was elongated and the spin was about the longitudinal axis. This configuration is shown inside the bulbous fairing in Fig. 3. The moment of inertia about any transverse axis is greater than that about the longitudinal axis, and it is known that such a body spinning about its long axis is not stable, but develops a wobble or nutation which increases with time. The rate of increase approaches zero for a very rigid body, but becomes significant for a coupled composite body with internal friction.

---

[1] Approximate orbit parameters were:

Inclination, deg	57.62	Apogee, mi	530
Period, min	95.6	Perigee, mi	155

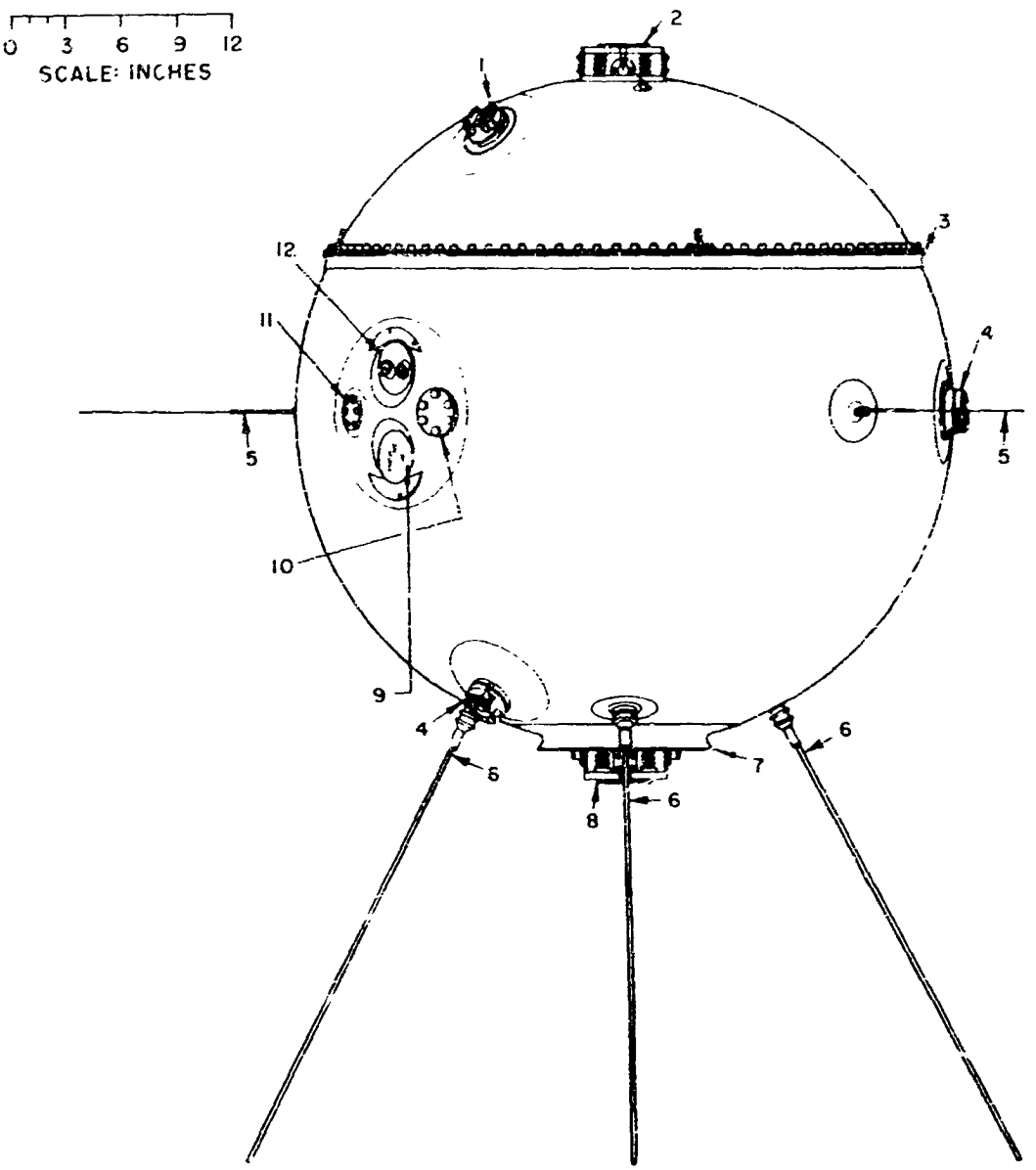

(1) REDHEAD PRESSURE GAGE
(2) UPPER MASS SPECTROMETER
(3) MAIN JOINT
(4) BAYARD-ALPERT PRESSURE GAGE
(5) ELECTRON TEMPERATURE PROBE
(6) R F ANTENNAS
(7) ATTACHMENT FITTING
(8) LOWER MASS SPECTROMETER
(9) SUN-MOON ASPECT SENSOR
(10) ELECTRICAL CHECK-OUT PORT
(11) PRESSURE PORT
(12) EARTH ASPECT SENSOR

FIG. 1. NASA S-6 Atmospheric Structure Satellite.

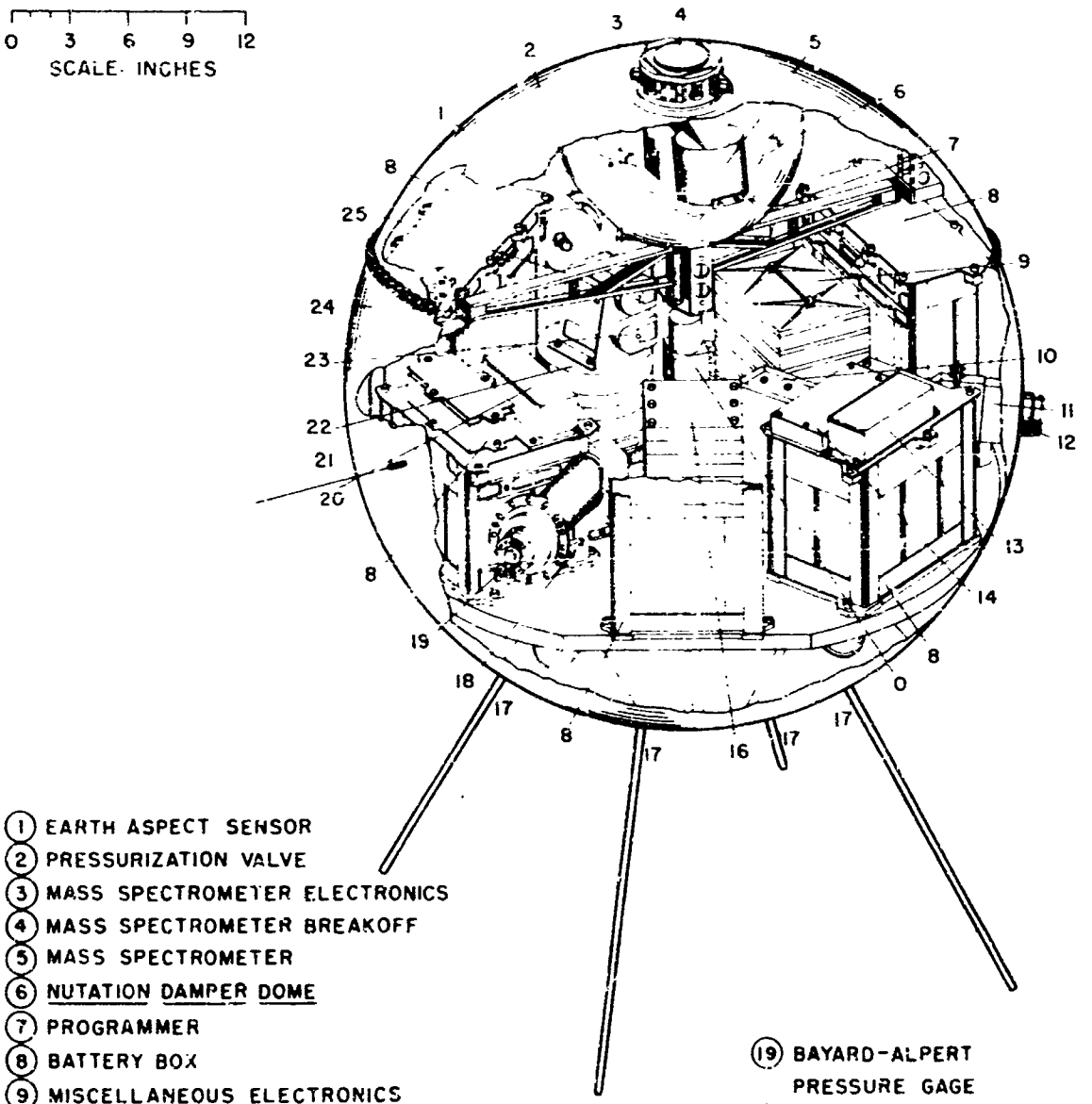

FIG. 2. NASA S-6 Atmospheric Structure Satellite Instrumentation.

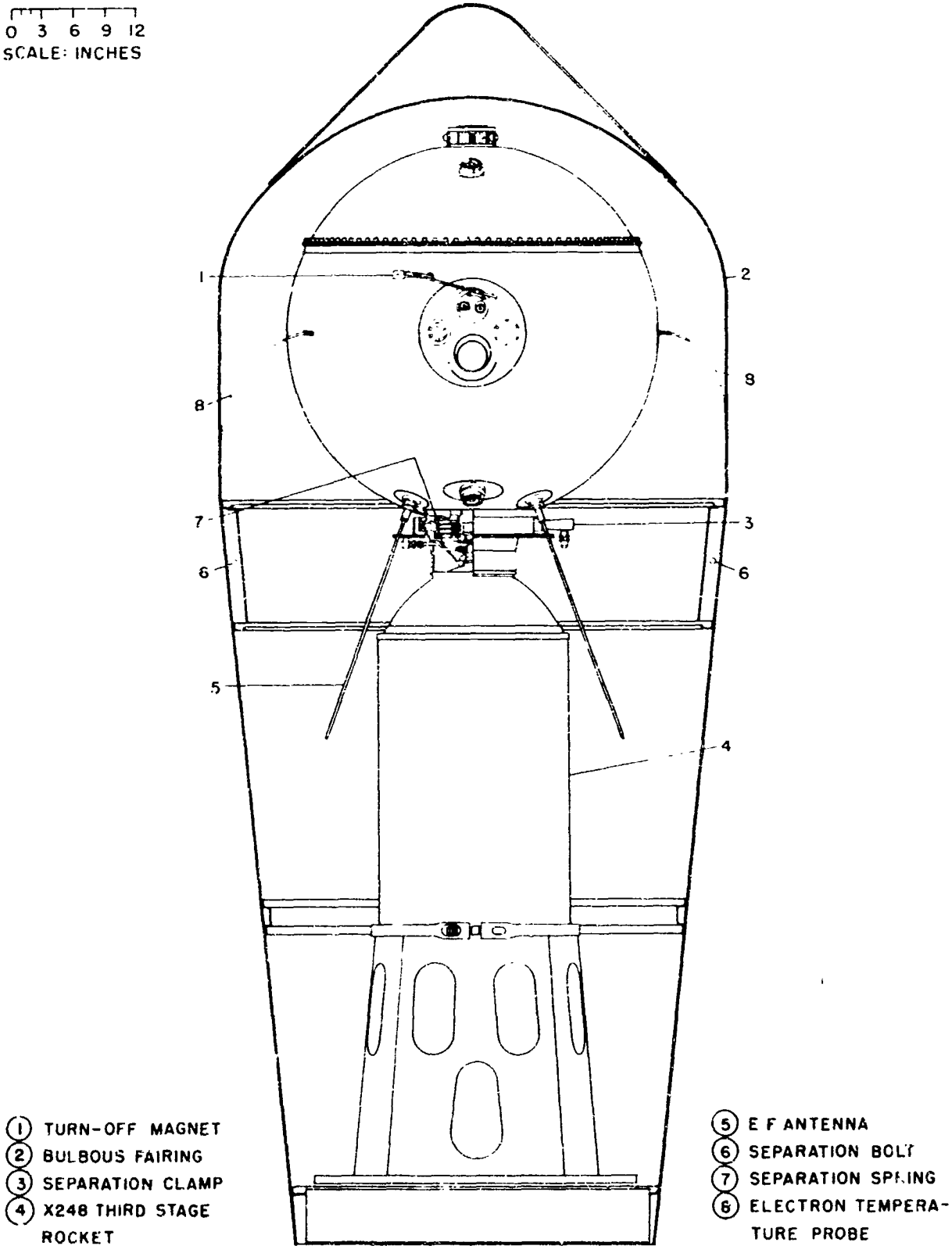

FIG. 3. NASA S-6 Satellite Third-Stage Assembly.

The thrust period of the last booster was about 38 seconds, a time probably too short for a significantly large yawing motion to build up in the heavy projectile, even though there should be fairly large thrust misalignment. However, because after-burning bursts were a probability, it appeared necessary to keep the spent booster attached to the satellite for a period of about 1,500 seconds, or 25 minutes, after the end of thrust. This period was long enough for a significant nutation of the assembly to develop even though the assembly was kept as rigid as possible. After separation from a spent motor, a satellite will retain nutation and may even receive an additional kick during separation.

Data, taken by instruments in the satellite, were expected to have a modulation at the spin frequency. This modulation would be uniform and easily accountable if there were no nutation or wobble of the axis and if any precession, resulting from outside torques, were slow. Otherwise, any significant amount of nutation would make data reduction confusing and difficult. It was therefore necessary to damp out the nutation expected, and this had to be done as soon as possible so that usable data could be gathered without delay.

Following a review of theoretical and experimental research studies in spinning body dynamics, carried out at the Naval Ordnance Test Station (NOTS), NASA requested that this Station develop, design, and fabricate a nutation damper for the NASA Atmospheric Structure Satellite, S-6.

With the S-6 satellite requirements in mind, the objective of the project can be defined as that of developing, designing, and fabricating the best possible nutation damper mechanism which:

1. Would be passive, injecting no material into the atmosphere about the satellite, and requiring no power to operate;

2. Could be clamped while the satellite was attached to the booster so that during this period, the assembly would be as nearly rigid as possible; and

3. Could be released upon radio command to provide fast nutation-damping after the satellite was in orbit.

The associated, or implied, project requirements were:

1. To specify the limits for the moments of inertia of the satellite so that fast nutation-damping was possible;

2. To collaborate with NASA in the specifications for the damper mechanism weight, location, mounting, and space requirements in the satellite; and

3. To show the effect of the various parameters of the satellite and damper on the nutation-damping characteristics.

This project objective and the details of the plan of approach were delineated in a "Project Plan"[2] by NOTS and a "Specification"[3] by NASA.

This report documents the over-all effort in the assignment, describing the pendulum-type nutation damper, and giving the design study history which includes discussions of the experimental small-model and full-scale laboratory model simulators, and of tests performed in each phase of the development. Appendixes A and B give additional details found useful in the adjustment of the pendulum hinge-friction coefficient. Appendix C expands briefly the criterion for pendulum tuning.

GENERAL DESCRIPTION

The pendulum-type damper for the S-6 satellite consists of two identical pendulum arms supported in a rigid framework that holds them in accurate relationship to each other and to the satellite body. These two diametrically opposed arms are free to swing through large arcs in a plane which is normal to the satellite spin axis and is displaced from the center of gravity (c. g.). Figure 4 (a) shows one pendulum arm clamped by the caging box while the other pendulum is free to swing. In Fig. 4(b), both pendulum arms are shown clamped in diametrically opposed positions, as would be assumed during boost. Table 1 lists the BuWeps drawings which give detailed design information.

The pendulum hinge-pins, spaced one inch apart, are so mounted in the satellite that the spin axis passes exactly midway between them. Although better tuning for more effective nutation damping might have been obtained had this spacing been narrower, the wider spacing had two advantages and therefore was selected and fixed early in the development. One advantage is that this spacing allows sufficient room for an effective viscous-friction generator for the hinges which are a critical part of the damper. The other advantage is that wider hinge-pin spacing permits greater errors in damper placement and in satellite dynamic balancing before unbalancing effects become serious.

---

[2]U. S. Naval Ordnance Test Station. Atmospheric Structure Satellite (S-6), Dynamic Stability Study, by Aeromechanics Division, Weapons Development Department. China Lake, Calif., NOTS, 19 February 1960; Rev. 1, 15 November 1960; Rev. 2, 20 October 1961. (Project Plan No. 4065-1.)

[3]National Aeronautics and Space Agency, Goddard Space Flight Center. Specification, Atmospheric Structure Satellite (S-6), Program for Dynamic Stability Investigation, by Mechanical Systems Branch, Payload Systems Division. Greenbelt, Md., NASA, 14 March 1960. (NASA Specification No. 94-6.)

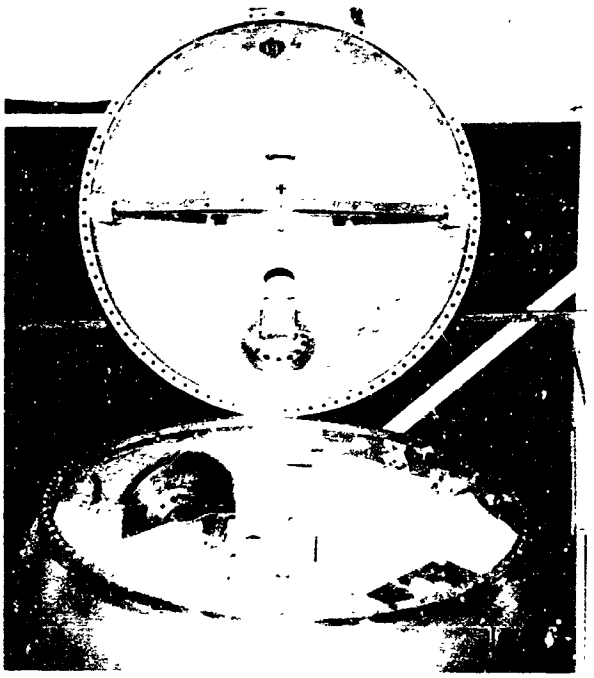

(a)

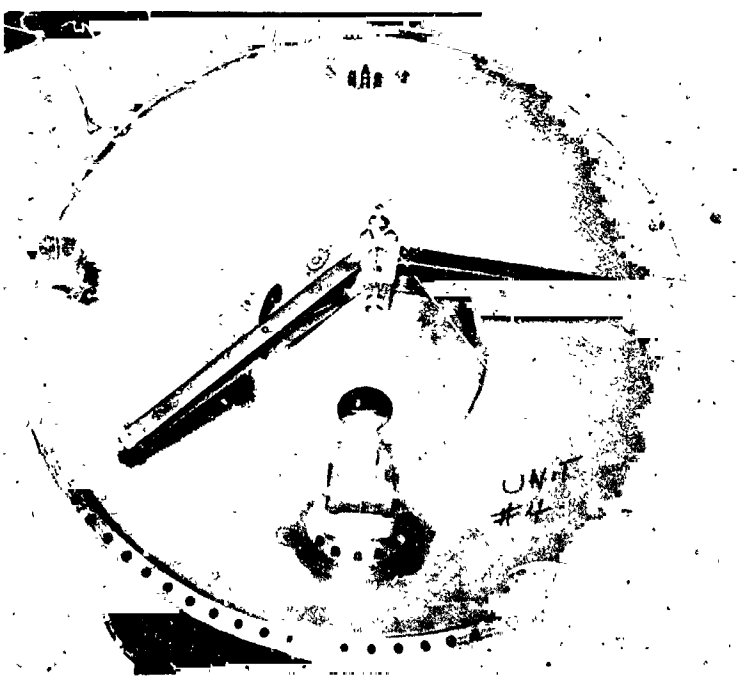

(b)

FIG. 4. Nutation Damper in No. 4 Prototype of NASA S-6 Satellite.

TABLE 1. Bureau of Naval Weapons List of Drawings: Pendulum Nutation-Damper for NASA S-6 Satellite (LD 448151)

Part	Drawing No.	Size
Pendulum Damper Assembly	SK 564012	D
Spindle Assembly	SK 563904	C
Spindle	SK 563907	B
Retainer	SK 563905	B
Outer sleeve	SK 563909	C
Inner sleeve	SK 563908	B
Outer spacer	SK 563906	B
Shimming ring	SK 563921	B
Pin	SK 564011	B
Ball bearing, New Departure RS 77R4D		
Tip Assembly	SK 564013	B
Retaining ring	SK 563911	B
Cap	SK 563928	B
Socket	SK 563922	B
Body, pendulum tip	SK 563914	C
Shim	SK 563912	B
O-ring, AN6227-1		
Caging Unit Assembly	SK 564037	C
Body	SK 563925	C
Cover plate	SK 563924	B
Head plate	SK 564243	C
Pin	SK 563923	B
Spring	SK 564242	B
Mounting bracket	SK 563927	C
End plate	SK 564041	B
Telescopic piston actuator, Atlas Powder Company Dwg. No. 1 MT 111		
Shear wire (solid annealed copper, resin-covered, round magnet wire) No. 27 AWG		
Frame, side plate	SK 563917	B
End plate	SK 563916	C
Base plate	SK 563918	C
Stiffener	SK 563919	C
Washer	SK 563920	B
Arm	SK 563915	C

The pendulum arms were fabricated from 0.033-inch-thick 24T3 aluminum, bent to form shallow channels and to obtain light-weight but strong stiff members. At the suggestion of the NASA representative, internal bracing (which formed small triangles) was installed within the arm structure to increase stiffness in the satellite axial direction.

The pendulum bobs are made of brass to provide as much weight as practicable at these extremities and, consequently, the greatest possible effective arm length. For faster nutation damping, a heavier strong material such as tungsten could have been used (lead was considered to be too soft). However, since the damping rate was satisfactory, a heavier material was not necessary. Provision was made for adjusting the positions of the extreme pendulum-bomb tips to engage the T-pin of the caging device. The caging boxes are easily distinguished in Fig. 4 and are shown fastened to the upper hemisphere of the satellite.

PENDULUM HINGE

Since both analysis and model experiments showed the friction in the pendulum hinges to be probably the most important parameter in the nutation-damping process, particular care was given to hinge development. The objective was to obtain a fairly large amount of purely viscous friction with as little as possible static starting or coulomb friction. The theory assumes the frictional torque to be proportional to the first power of the angular velocity of the pendulum arm about its pivot. For this application, it was necessary only that torque approach zero as relative angular velocity approaches zero.

The reasons for this are simply stated. If static friction were present, the chance would be high that the pendulums would reach final stationary positions displaced from the diameter through the hinge pins. That is, the angles, φ, between the pendulums and their equilibrium positions would not reduce to zero when nutations were damped out. This condition would cause a dynamic unbalance of the satellite, which, of course, was undesirable. Since the satellite spins slowly, 1.5 rps, and since the pendulum hinge-pin is close to the spin axis, the pendulum restoring torque is low; and even small amounts of static hinge-friction could result in large final displacement angles, φ, from the equilibrium position. The form or nature of the frictional torque in other respects is not critical since the very fastest possible nutation damping is not required. Further study, involving nonlinear mechanics, might reveal the optimum form for the viscous frictional characteristic.

In the first models of the pendulum hinges, sleeve bearings were used and favored because they were simple and rugged. The bearing having the largest outside diameter compatible with the available space (1-inch pin separation), was used. In one case, coarse screw threads were cut the length of the bearing to increase the wiping surface area.

In another case, specific bearing bands approximately one-half-inch wide were provided at the ends of the 3-inch-long bearing sleeve. In these bands, the clearance was less than that in the center section. However, these sleeve bearings did not show consistent performance in oscillating pendulum-like motions. Particularly after long stationary periods, the change in friction was high. Therefore, effort was directed toward ball-bearing designs.

In ball-bearing hinge design philosophy, ball bearings take the load of the pendulum and hold the other hinge parts in proper relation to each other. Figure 5 shows a cross section of the hinge assembly. The center spindle is fixed in the nutation-damper framework in a manner that clamps the ball-bearing inner races in place. The distance between these inner races is adjusted by shimming rings to produce a very light or zero axial bearing preload. The distance between the outer races of the bearings is determined by the cylinder (labeled outer sleeve in the figure), which has two lugs on one side for attaching the pendulum arm. With only these described components, the pendulum will rotate with extremely low friction of either a static or viscous type.

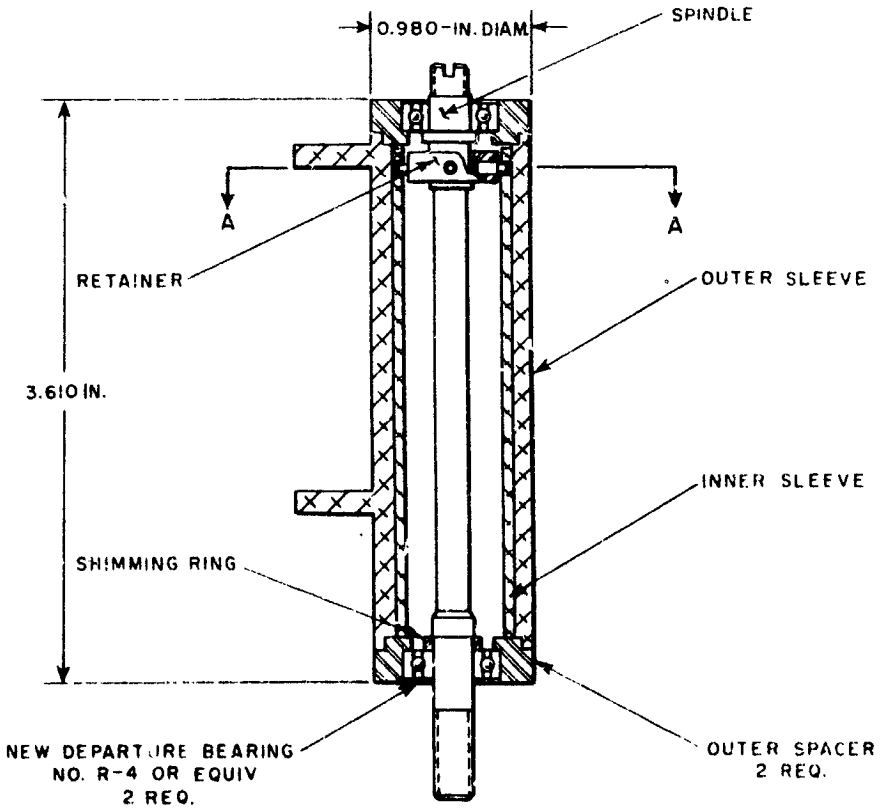

FIG. 5. Pendulum Hinge Assembly.

To produce a controlled amount of only the viscous-type friction, the cylinder (labeled inner sleeve) was added, and, of course, was not allowed to rotate with the pendulum. There was ample end clearance (0.020 inch) for this cylinder. However, the outside diameter of the sleeve was 0.747, +0.000 and -0.001 inch; the inside diameter of the outer sleeve was 0.750, +0.001 and -0.000 inch so that 0.005-inch-maximum and 0.003-inch-minimum radial clearance between the cylinders were expected. Under normal or even superior shop practice, the clearances can exceed these limits because slight ellipticity and non-straightness in the cylinders may be caused by warpage of the aluminum material, or by the load of the pendulum arm. The clearance specified, however, was sufficient to insure entirely free rotation of the outer sleeve about the inner sleeve. The desired viscous friction is produced by filling the space between cylinders with fluid of selected viscosity.

In the first model ball-bearing hinge, the inner sleeve was held rigidly in position with respect to the spindle. Close tolerances on the bearing seats and the spacers were expected to maintain sufficiently good concentricity of the inner and outer sleeves to prevent contact between them. This did not work, however, and a floating mount for the inner sleeve was used (Fig. 6). This adaptation of a flexible torque-transmission coupling permits the inner sleeve to shift sideways and to tip slightly in any direction, without permitting any significant amount of rotation about its longitudinal axis. Thus, the inner cylinder is free at all times to center itself and also to align itself with the outer cylinder, yet the sleeves cannot rotate together.

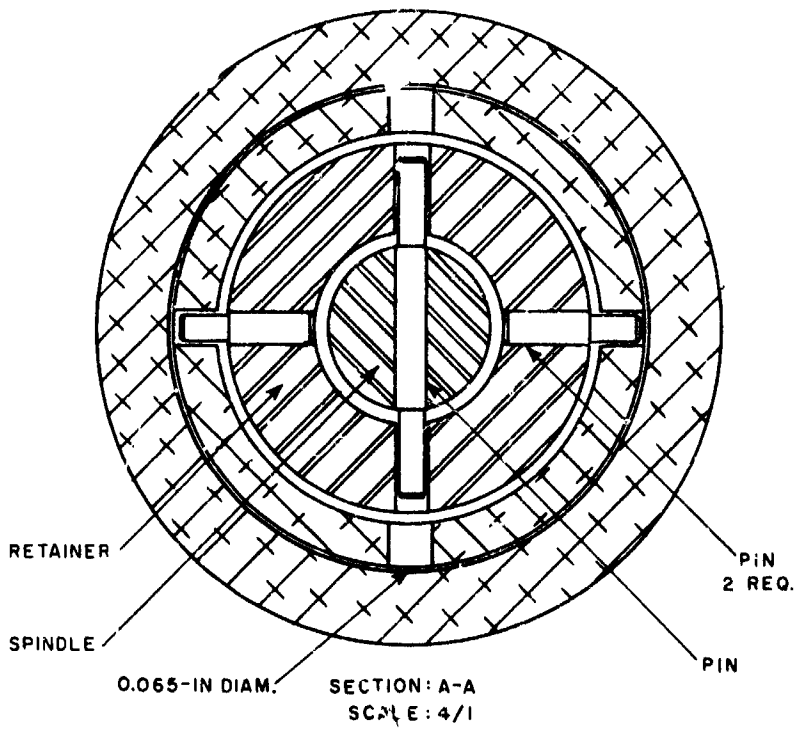

FIG. 6. Floating Mount for Inner Cylinder of Pendulum Hinge.

Dow Corning "200 Fluid," used to provide the viscous friction, is a silicone fluid available in a great range of viscosities, from 0.65 to 2,500,000 centipoise (cp). Full-scale simulator tests indicated that a viscosity of 2,400 centipoise is nearly optimum for the S-6 satellite application. The fluid was introduced carefully into the very narrow space between the inner and outer cylinders so that no bubbles or unfilled areas would be present. Any excessive fluid was allowed to drain away. The surface tension of the fluid, in the narrow open annular areas between the sleeves at the top and bottom, is the mechanism for retention of the damping fluid. Thus, the static friction normally introduced by oil seals is not present.

Even under the worst environmental conditions, the ball bearings do not approach their load limits. Before use, they were cleaned and lubricated with a small amount of light-weight watch oil. This oil has low-migration properties and provides good lubrication under low speeds and high pressures.

This ball-bearing hinge gave consistently excellent results. Negligible static-friction and desired viscous-friction were maintained even after months of storage.

UNCAGING MECHANISM

The U. S. Naval Ordnance Test Station undertook the problem of clamping or caging the damper pendulums until the satellite reached orbit and was free from all booster motors. Originally, it was not understood that this problem was part of the NOTS participation. However, as time for this step in the program approached, it appeared that it could be done most expeditiously at NOTS.

The concept for the original caging-unit design included a mechanism for recaging the pendulum arms after they had once been released. If, for example, there were an accidental weight shift in the satellite, causing an unbalance, recaging the arms would minimize the unbalance effect. The recaging would take place after nutation had damped so that the change, caused by recaging, would induce a minimum of new wobble. Such an uncaging and recaging device was designed but not built. The design was quite complicated, and the NASA representative felt that the probability of a need to recage was negligible. Therefore, the objective was changed to design a more simple device for uncaging only.

In the beginning to avoid further modification of the satellite shell structure, it appeared advantageous to mount the caging mechanism on or to make it an integral part of the pendulum-unit framework. The general design idea of the device is shown in Fig. 7. A working model of this releasing mechanism was designed and fabricated at NOTS and then demonstrated at the Goddard Space Flight Center for the NASA representative. From subsequent consultation, it became evident that the problem of additional mounting structure on the satellite was minimal. Thereafter, emphasis was placed on reliability and redundancy in an actuation mechanism employing parts mounted near the satellite skin.

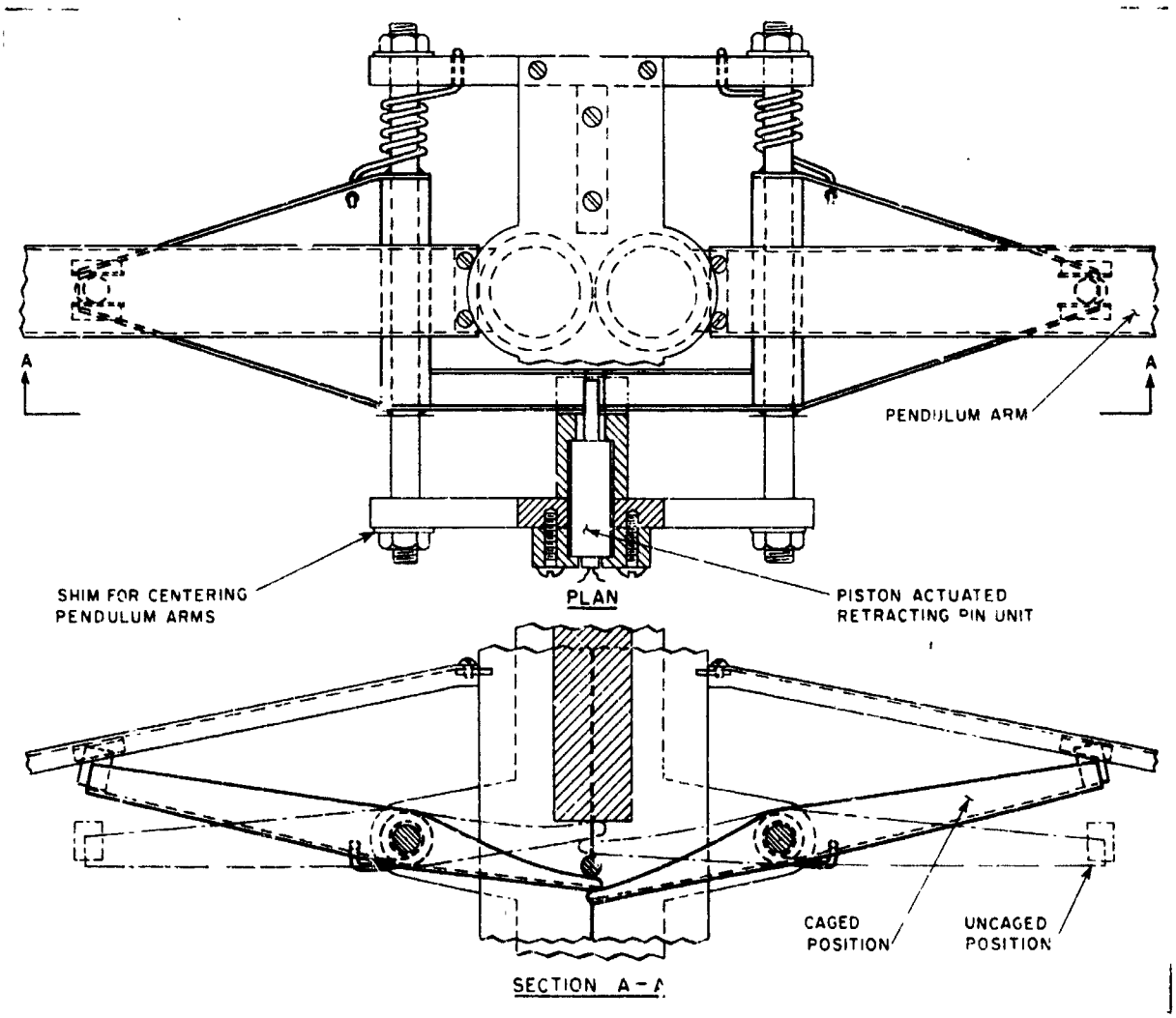

FIG. 7. Nutation Damper Caging Device No. 2, Partial Assembly.

The uncaging device, as finally developed, consists of a separate unit for each pendulum arm fastened to the satellite shell (Fig. 4). The pendulum bob is supported against all accelerations normal to the pendulum arm, thereby relieving much strain from the hinge bearings during the boost period. The mechanical advantage is good, both for supporting purposes and for positioning accuracy while the pendulums are caged. Finally, four squib-actuated pistons were used in a manner such that if any one of them functions, at least one pendulum arm will be released, thus providing adequate nutation damping.

The caging box (or unit) contains these squib-actuated pistons, and a caging pin and bar made of one piece of metal formed in a T. The caging pin extends from the unit to engage the socket at the extreme tip of the pendulum bob, as may be seen in Fig. 4(b). The pin is retracted by the two pistons which push against the T-bar at the other end of the caging pin when a remotely controlled signal is given. If either of the actuating pistons function, the pin will retract. Figure 8(a) shows a unit with the caging pin protruding from the box toward the pendulum-bob tip socket, which the pin engages when caging is desired. In Fig. 8(b), the complete assembly is shown with pin retracted and piston actuators extended.

The piston actuators are electrically initiated pyrotechnic devices; each has a diameter of 0.313 inch. In closed position, the actuator length is 0.75 inch, and in opened position, each actuator is 1.313 inch long plus about 0.06 inch allowance for wires. The bridge wire resistance is about 1 ohm, maximum. None of the actuators will fire at 0.1 ampere, and all will fire at 1.0-ampere current. Thrust exerted is from 15 to 20 pounds, and the functioning time is about 14 milliseconds. As may be noted in Table 1, the piston actuators are specified as Atlas Powder Co. Drawing No. 1 MT 111.

Although the piston rods strongly resist retraction after firing because little or no gas escapes from inside the piston, a spring-loaded catch, a part of the caging box, insures that the caging pin is held in the retracted position.

To eliminate rattle or to take up play in the motion of the pin, neoprene O-rings are used both inside the caging unit and in the pendulum-bob tip socket. The O-ring in the caging box is near the outside end of the pin so that the shoulder portion of the caging pin is caught behind the ring in the retracted condition. This provides an additional safeguard against caging-pin interference after retraction. Although severe vibrations during boost were expected, smooth orbital conditions were anticipated, hence, rattling after uncaging was not considered to be a problem.

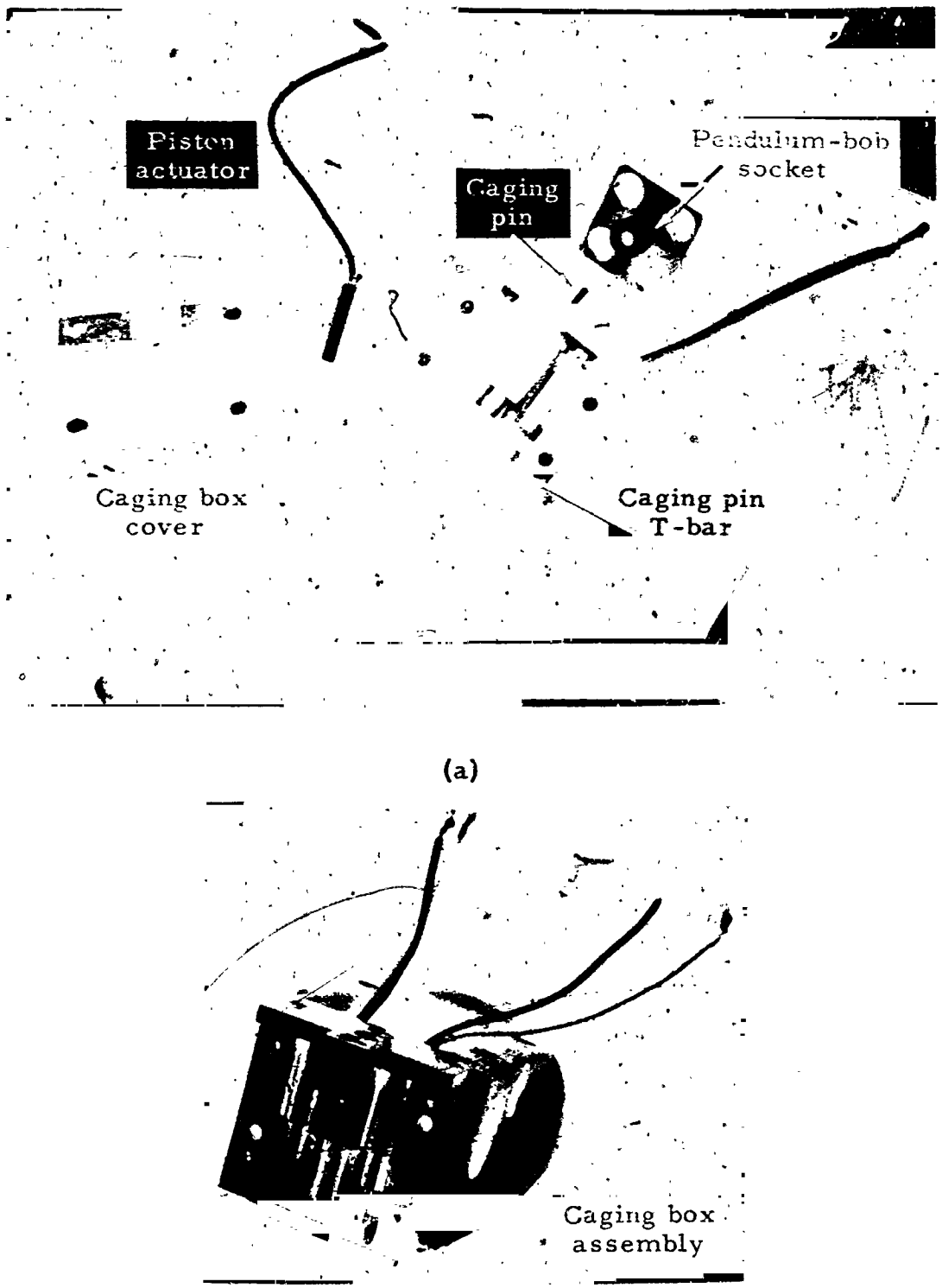

FIG. 8. Caging Box Components, Showing (a) Piston Actuator, Caging Pin and T-Bar Positioned Before Actuation, and (b) Caging Box Assembly Positioned After Actuation.

The final feature of the caging-box design is the shear wire intended to prevent accidental caging-pin retraction before the piston actuators are fired. Extensive bench tests were made in which several sizes of wire were sheared under measured loads. Resin-covered, annealed-copper magnet wire was selected as the most uniform, readily available material for the purpose. The tests showed that the No. 27 wire, specified, would hold consistently at a 10-pound load and break at 12 pounds. In these tests, force was applied slowly to the wire, and the test table vibrated in varying amounts because air-conditioning machinery was nearby. Nevertheless, the load test results were all within the figures given. Since the presignal load to break the wire was expected to consist of inertial forces of the 0.03-pound caging-pin under possible 12-g accelerations and since the minimum shearing force from a single piston actuator was 15 pounds, applied with considerable shock, it appeared that the shear wire was adequate.

In all bench tests made during the caging mechanism development, there were no failures of the pin to retract. In some cases the pendulum arm was set at an angle to cause binding of the pin in the pendulum-bob socket hole; even then, release action was positive. One necessary modification was to increase the strength of the box end-plate. Upon retraction, the caging pin T-bar strikes this end-plate. In an early test when two actuators were fired simultaneously, the box end-plate bent slightly. For this reason, it was made thicker at the center, increasing the plate strength without increasing the space required for the caging box. In subsequent tests, no bending was observed. Figure 4 shows the caging box mounted against the curve of the upper hemisphere ring in the satellite.

PLACEMENT AND DIMENSIONAL LIMITATIONS

A close examination of Fig. 2 will show, in general, where the nutation damper is located in the satellite. It may be seen that although much space is allowed for the damper assembly, there are limitations. These limitations are better indicated in Fig. 9; here ample room is shown near the center and downward inside of an 8-inch-diameter cylindrical space, but outside of this area, there are obstructions extending to the skin at a distance of 6.5 inches up from the satellite equator, as indicated by the dashed lines in the figure.

The nutation damper is mounted from above to a hemispherical, or dome-like support as shown. This support (designed by the Budd Company, contractor for designing and building the sphere) is required to hold the damper rigidly on the centerline of the satellite and, at the same time, to leave room for a mass spectrometer at the top center of the upper hemisphere. The plane of the supporting platform is 9.25 inches above the equator, leaving a clearance of 2.75 inches for the pendulums. A further restriction is that the swing of the pendulum arms be limited so that when they approach each other on either side, the minimum angle between them is 20 degrees.

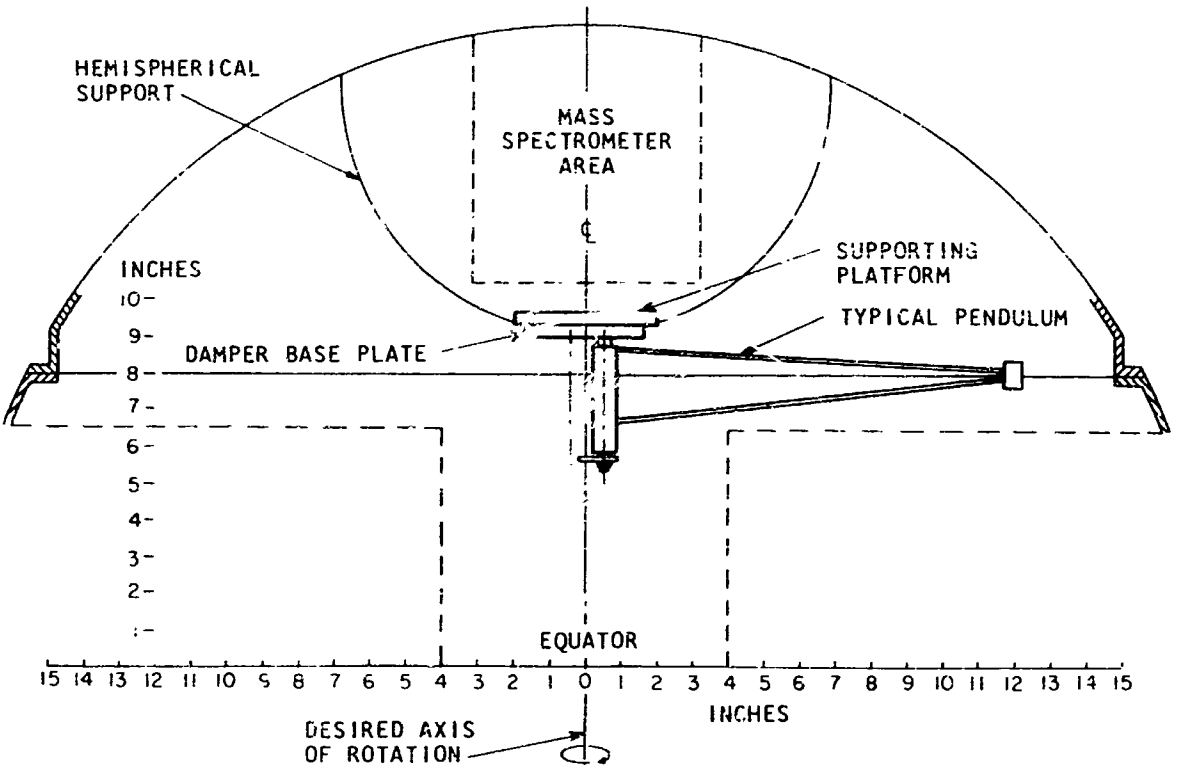

FIG. 9. Space Allowance for Nutation Damper.

The nutation damper assembly is bolted to the supporting platform by four screws at the corners of a 2.50-inch square, laid out on a plane at the bottom of the dome-like support. Tolerances are loose for the positions of the screw holes, but they are close for a 0.125-inch-diameter locating pin in the center of the square (see BuWeps Drawing No. SK 563918). This locating pin in the damper assembly base plate is positioned accurately with respect to the pendulum-hinge axes, and the damper assembly hemispherical support platform has the mating hole positioned accurately with respect to the satellite symmetry axis. This hole was located and drilled after installation of the mount in the satellite, and precise measurements to points on the satellite upper hemisphere connecting-ring were made. Only one locating pin was necessary since changes in rotational position did not affect damper operation, and the only other problem was interference with other contents of the satellite.

ENVIRONMENT

The atmospheric environment for the nutation damper when the satellite was in orbit, was expected to be little different from that of standard atmosphere at sea level on earth because the damper would be entirely enclosed in the hermetically sealed stainless steel sphere.[3] It was anticipated that the atmosphere would be air at about 15 pounds per square inch of pressure as long as the temperature was also normal, and it was calculated that this should be the case when the satellite was in the shadow of the earth a significant part of the time. These conditions greatly simplified the problem of lubrication in the pendulum hinge-bearings and the means for obtaining and controlling viscous hinge-friction.

The acceleration and vibration environment in orbit is much more favorable than at earth surface because effective gravity is zero during orbit, but during the boost stages, the environment is much more severe. The following table shows the conditions.

Acceleration:	
Axial, g	22.0
Laterial, g	1.0
Rotational (polar axis), radians/sec^2	29.0
Vibrational, g:	
5-25, cps	2[a]
25-100, cps	4
100-700, cps	6
700-1,000, cps	12

[a]Except as limited by 0.4-inch double amplitude.

The nutation-damper pendulums, hinge bearings, and caging mechanism required particularly rugged designs because of these conditions.

DESIGN STUDY HISTORY

Prior to the attack on the problem of NASA S-6 satellite nutation-damping, there had been studies at NOTS on various damping mechanisms known to affect nutation type of motion in gyroscopes and freely spinning bodies. Problems had arisen in connection with spin-stabilized sounding vehicles and other projectiles traveling in very thin atmosphere. Moreover, the action of a mercury nutation damper, effectively used in the Sidewinder missile-seeker system, was not understood thoroughly enough to apply its design principles with confidence to other applications. Therefore, a basic approach to understanding the problem of passive control of this free oscillatory motion appeared to be needed.

SMALL-MODEL TEST VEHICLE

First, a model test vehicle was designed and fabricated in order to perform experiments easily. This model was the Space Vehicle Dynamical Simulator, shown in Fig. 10. It consisted essentially of two heavy bronze disks that were screwed onto a cylindrical aluminum body. The relative positions of these disks determined the ellipsoid of inertia of the simulator. The range of the ratio of polar to transverse moments of inertia was 0.75 to 1.55, approximately, and adjustment within this range was quick and easy.

FIG. 10. Small Model Test Vehicle.

A thin steel spike, protruding from one end of the cylinder, defined the symmetry axis and facilitated observation of the motion. This spike and a few small tapped holes placed symmetrically in the disks and body simplified attaching experimental devices as they were conceived.

Bearings

The space within the cylindrical body was used for a universal bearing mount, the design of which permitted unlimited rotation about the symmetry axis and approximately ±20 degrees about any transverse axis. This bearing was, of course, a very critical part of the simulator. Friction had to be low, but more important, the friction in transverse rotation could not be higher than in polar rotation or spin.

Two types of bearings were used in this test vehicle. The first, a simple spindle design, is indicated in Fig. 11. The conical tip of the spindle (a continuation of the spike on the centerline of the cylindrical body) rested in a small cup made of steel or sapphire material, fixed to the end of an upright support. The cup was a hollow cone with the tip truncated, in one case by a tangent spherical surface of about 0.015-inch radius, and in another case simply by a plane of about 0.020-inch diameter. The tip of the steel spindle was hardened and carefully ground to a tangent sphere with a radius of about 0.010 inch. The included angle of the cup was 90 degrees and that of the spindle was about 40 degrees.

For the second type of bearing, a small three-axis gimbal system was used. It was borrowed from the seeker system of a Sidewinder 1-A missile. Six miniature ball bearings provided exceptionally low friction when almost all of the bearing preload was removed. This ball-bearing mount was less easily damaged than the spindle and jewel bearing. It was felt, however, that the lowest friction in all three axes could be obtained with the spindle design.

Other bearings were considered but not built. In particular, there were plans to construct a fluid bearing in which light oil could be pumped up through the support shaft to the space between spherical bearing surfaces and allowed to run back down to a sump. An air (or gas) bearing also was considered. However, all of these bearings involved much additional apparatus for what appeared to be small gain. It was realized, also, that such refinement could lead only to other limitations such as those imposed by spinning in dense atmosphere on earth, instead of near vacuum at high altitude.

Mount

Finally, the upright shaft supporting the bearing was set into a heavy brass base. During operation care was necessary to set this base, so that it would not rock, on a stable laboratory table. Ideally, in space

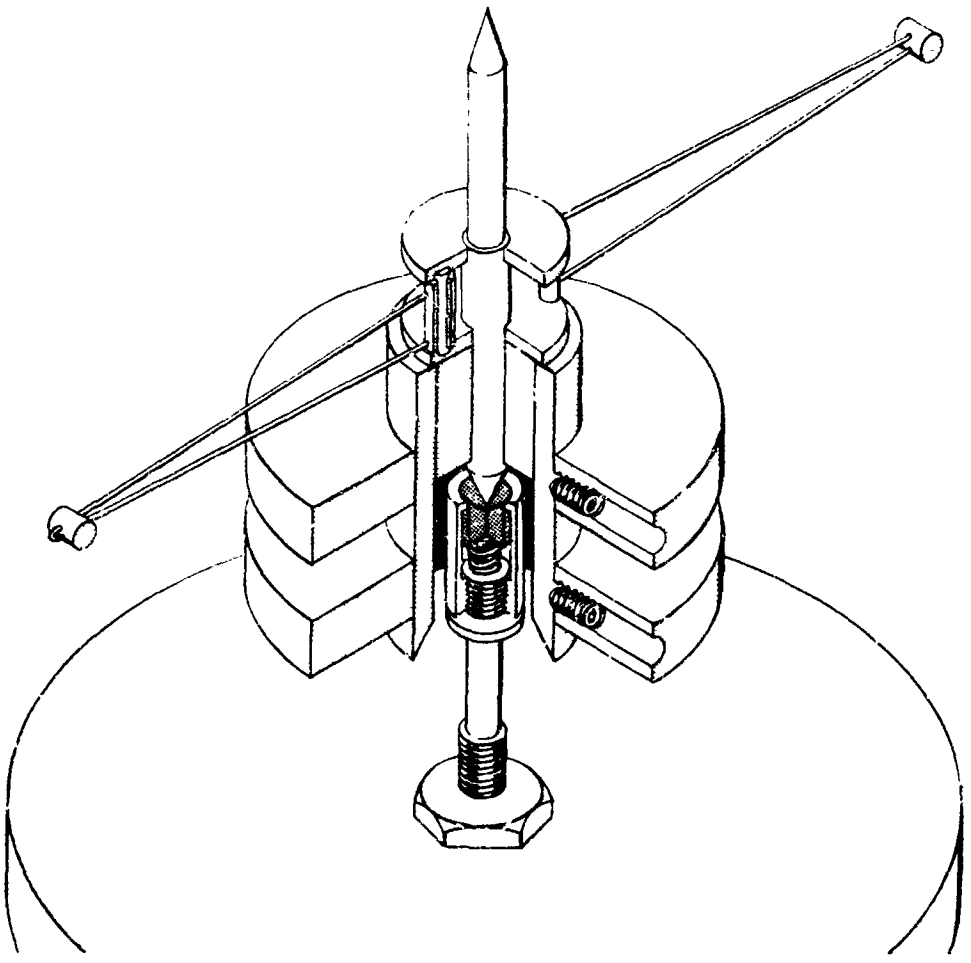

FIG. 11. Spindle and Jewel Bearing.

simulation there would be only vertical forces on the support even with the simulator spinning. However, if the disks should be adjusted so that the c. g. of the simulator is not exactly at the center of the universal bearing, there would be side forces. Then, if the support should rock, there would be accompanying energy dissipation and nutation damping would be strongly affected.

Spin-Up and Spin Decay

The simulator was spun twirling the spindle between the thumb and forefinger. A three sixtenths-inch-diameter spindle was chosen after some consideration, and it appeared large enough to supply the leverage required to accelerate the heavy disks rapidly, yet it was small enough to obtain a maximum speed of 10 or 12 rps (600 or 700 rpm). This speed was fast enough to cause the centrifugal acceleration near the rim of the disks to be about twenty times gravity. After spin-up, with reasonably good bearings the simulator would coast for about 20 minutes without stopping. Since most of the experiments could be conducted in a minute or less, spin was considered constant during a test.

FIG. 12. Test Vehicle Data at 64 Frames/Sec.

The speed of the simulator was determined by synchronizing a General Radio Strobotac with the spin rate. The "strobe" was also synchronized with the nutation rate by stopping the spindle motion. The ratio of the latter flash rate to the former gives the polar-to-transverse moment of inertia ratio.

Observation of Performance

Measurement of the performance was accomplished in several ways. When the spindle was lighted and viewed from the side against a dark background, the motion of the sharp tip was evident in good contrast. There was no difficulty arriving at a qualitative conclusion as to whether a nutation was damped or undamped; moreover, even a slow precession (the motion resulting from an outside torque) was easily observed.

To obtain quickly an approximate measure of the nutation-angle rate of change, a mechanic's steel rule was clamped horizontally to an adjacent stand. Then by quickly positioning the steel rule to about one-eighth of an inch above the spindle of the spinning nutating simulator, the measurement of nutation amplitude could be made to within about one-twentieth inch. The change with time was determined by using a stopwatch.

For observation of fast changes covering less than a few seconds, or for greater accuracy or more detail (such as position of damper components), moving pictures were taken with a 16-mm camera placed directly above the simulator. Camera speed of 64 to 100 frames per second was sufficient, providing six to ten pictures per turn of the model. To obtain sharp individual images, a camera shutter angle of 6 degrees was used. Two No. 6 flood lamps provided ample light for fast, black and white film (Eastman Tri-X, Pan.). A 3-second stopwatch in the field of view provided readings from which camera frame-rate could be checked or calibrated. Camera frame-rate, assumed to be constant over the few seconds of observation, then provided the time base. A sample of such record is shown in Fig. 12.

Rigid Body Verification

As suggested in an earlier section, much significant experimentation can be done with less than perfect bearings. Since buildup or decay of nutation for a rigid body depends on the relative amounts of friction in the polar and transverse bearing axes, control runs should be made before and after any test. In these runs, the behavior of a simulator as a rigid body should be observed for various values of the moment of inertia ratio. By this procedure, one minimizes the chance of being misled by experimental conditions unknown to him. Furthermore, one can proceed with experiments using less elaborate equipment and therefore usually with less delay.

This model simulator then provided a means for easy, quick, and inexpensive testing of the various nutation-damper theories and subsequent design proposals. The model could be operated easily by one man with no need for a supporting crew. Even photometric work was possible without scheduling. Some of the devices or modified mechanisms for testing were handmade by the experimenter, mostly without machine tools. Other devices were made in a "first-model" shop from freehand sketches. At this scale, tolerances were nominal and hardware was easy to handle. Nutation-damper development was undoubtedly speeded by the use of these experimental models.

EARLY EXPERIMENTS

Early experiments with the test vehicles were directed toward fundamentals and simplicity of a dynamical model. Rigid-body performance was tested with various settings of the disks. For example, the ratio of polar-to-transverse moments of inertia, A/B, was varied while the c.g. was maintained as closely as possible at the universal bearing center. Nutation, or free-oscillation, performance was observed. Then with the c.g. displaced slightly from the support point, the free nutation was observed superimposed on the slow circular precession which was forced by the outside torque caused by gravity.

Single-Pendulum and Mercury-Drop Dampers

The first departure from a rigid body was a single pendulum, looped over the spindle of the simulator. Dynamically, this is more complicated than a second modification which was a small mercury drop

in a circular race, centered about the spin axis. The pendulum used was a spherical pendulum, one which was free to swing up and down as well as around the simulator; whereas, the mercury drop was constrained to move in the plane of the race. An attempt to analyze the problem with the mercury was made by A. V. Pratt.[4] Incidentially, a planar pendulum, which performed similarly to the mercury drop, was also made.

Both the mercury-drop and the pendulums damped nutation when the moment of inertia ratio, A/B, was greater than one, or undamped it when A/B was less than one. The action was erratic, sometimes fast and sometimes slow, as indicated by Pratt. However, after nutation was damped, there remained a small unbalance so that the model was not rotating about the axis of symmetry. Further, the orientation of this unbalance was unpredictable because it varied from one test to the next.

Unbalance Problem

To overcome this unbalance problem, the pendulum hinge, or pivot, was placed to one side of the symmetry axis of the simulator[5], and a counterbalancing weight was placed opposite it. This weight could be adjusted so that the equilibrium spin axis would be as close as desired to the symmetry axis. In equilibrium with nutation zero, a pendulum must be aligned along the radius through the hinge pin; static friction must be zero also or so low that the pendulum will not come to rest, appreciably, off this radial position. Note that this procedure of adjusting the weight is simply dynamic balancing.

Counterbalanced Offset Pendulums

It was a short evolutionary step to replace the counterbalancing weight with a second pendulum. This pendulum was hung from a pin, diametrically opposed to the first one. However, the pin was not required to be at the same radial distance as the first one, nor was it necessary that the pendulum lengths or weights be the same. All parameters were adjusted to produce dynamic balance in the equilibrium state when nutation was zero; alternatively, balance could have been obtained by adjusting weights fixed in the simulator.

This offset-pendulum arrangement is similar to the Frahm vibration damper described in Ref. 1, page 93. This reference states that a small mass is connected to a main rotating body in such a manner that the small mass vibrates at some natural frequency within the main body.

---

[4] U. S. Naval Ordnance Test Station. Theory of the Unsymmetrical Nutation Damper, by A. V. Pratt. China Lake, Calif., NOTS, 22 August 1959. (NOTS Technical Note 4065-63.)

[5] This had been suggested in an informal communication by F. H. Davis, Naval Ordnance Test Station, China Lake, California.

This natural frequency is matched or tuned to that of the unwanted vibration. The frictional resistance to motion between the large and small masses is adjusted until maximum damping of the undesired vibration is obtained.

Pendulum Tuning

In the early work with the nutation dampers, the tuning criterion was considered the most interesting feature. The possibility of an oscillatory property may be difficult to imagine when a weight must move in a circle, centered on the spindle of a simulator. However, a weight hung on a pivot, which is offset from the spin axis, can be pictured as having the oscillating properties of a pendulum. The force field is the centrifugal field instead of gravity, and a formula for the natural frequency and a resonance condition can be obtained.

In this case of the spinning space vehicle, the unwanted vibration is the nutation. The pendulum is in the spinning coordinate system and therefore "feels" only the difference between the spin and the nutation frequencies. For best nutation damping, therefore, it was reasonable to expect that the pendulum should be designed to resonate with this difference frequency. As shown in detail later, the pendulum frequency depends on pendulum length, L, the distance of the hinge pin from the spin axis, a, and the rate of spin. The nutation frequency is also directly related to the spin, specifically, by the ratio of moments of inertia, A/B (polar/transverse), and it is not surprising that the tuning of the pendulum to nutation is independent of spin. The simple tuning relation is:

$$\frac{a}{L} = \left[\left(\frac{A}{B}\right) - 1\right]^2$$

Stability

During initial attempts to check the tuning relation, the condition of "instability" was discovered. At values of the ratio of moments of inertia only slightly greater than one, the nutation frequency is only a little greater than spin, that is , the difference is small. For tuning, then, the pendulum must have a low frequency which requires that the pendulum arm be long or that the pin be close to the spin axis.

As extremes of these conditions were approached, it was found that the two pendulums of a balanced pair no longer settled to their diametrically opposed positions after the nutation had damped. Instead, they took fixed equilibrium positions at some angles, φ_1, φ_2 (Fig. 13), both on same side of the diameter through the pins. This, of course, created an unbalance so that the spindle continued to form a circle, as in nutation, about some spin axis other than the symmetry axis. It was

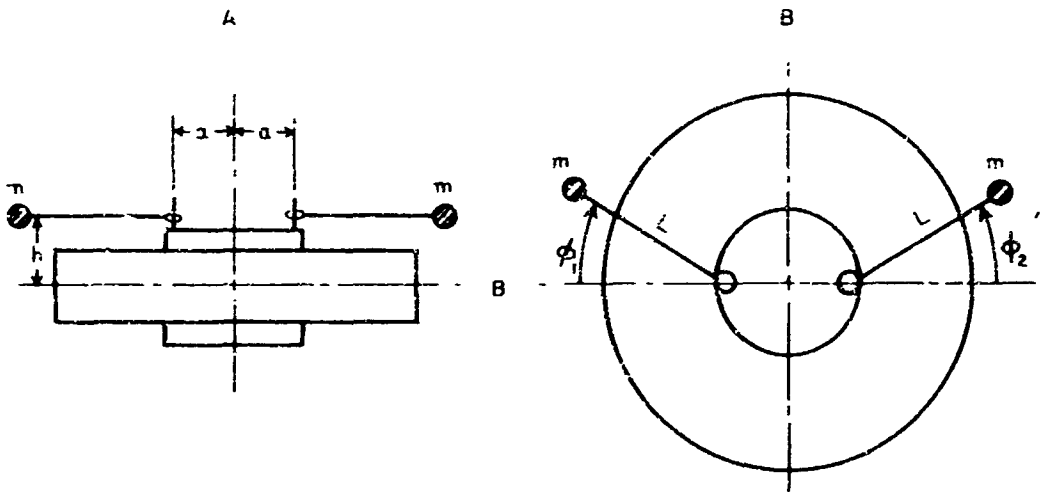

FIG. 13. Twin-Pendulum Nutation Damper.

determined that nutation was zero and that this was unbalance by noting that the spindle rotation-frequency was the same as the spin frequency. (In fact, in such a test, before nutation disappears, the size of the circle formed by the spindle tip increases and decreases periodically, as though the nutation and unbalance oscillations are beating with each other.) This undesirable condition of unbalance in the equilibrium condition, caused by the unaligned dampers, was disturbing and puzzling.

After observing this behavior, an analysis based on energy considerations was made by W. R. Haseltine (Ref. 2). A relation resulted, showing the conditions under which equilibrium deflection of the pendulums with the accompanying unbalance could be expected. The analysis was actually extended to a case of four symmetrically disposed pendulums, instead of two, and some experimental verification was accomplished with the simulator. The relation, simplified for the case of two equal pendulums (Fig. 13), is as follows:

$$\cos\varphi = \text{the lesser of } 1, \text{ or } S$$

where

$$S = \frac{(A - B)\,a}{2mh^2 L}$$

in which

A = polar moment of inertia of the symmetrical main body

B = transverse moment of inertia of the symmetrical main body

L = length of pendulum

a = distance from the main body axis to the pendulum hinge pins

h = distance from the c. g. of the main body to the plane of the pendulum hinge pins

m = mass of the pendulum bob

φ = equilibrium displacement angle between a pendulum arm and the diameter through the hinge pin

Again, after one knows that this equilibrium-unbalance condition exists, a simple geometrical derivation of the above formula is possible. In Fig. 14, the principal axes of the basic vehicle are represented by lines A, B, and B for the polar and the two (equal) transverse axes, respectively. The spin is about the axis A', rotated an angle, Θ, from A. This rotation is caused by the unbalance, shown at 2m in the diagram, which, in turn, results from the deflection of the damper pendulum bobs to angles φ. Note that the two pendulums fall on lines which cross at the stable axis of rotation, A', as they must since centrifugal force holds them there.

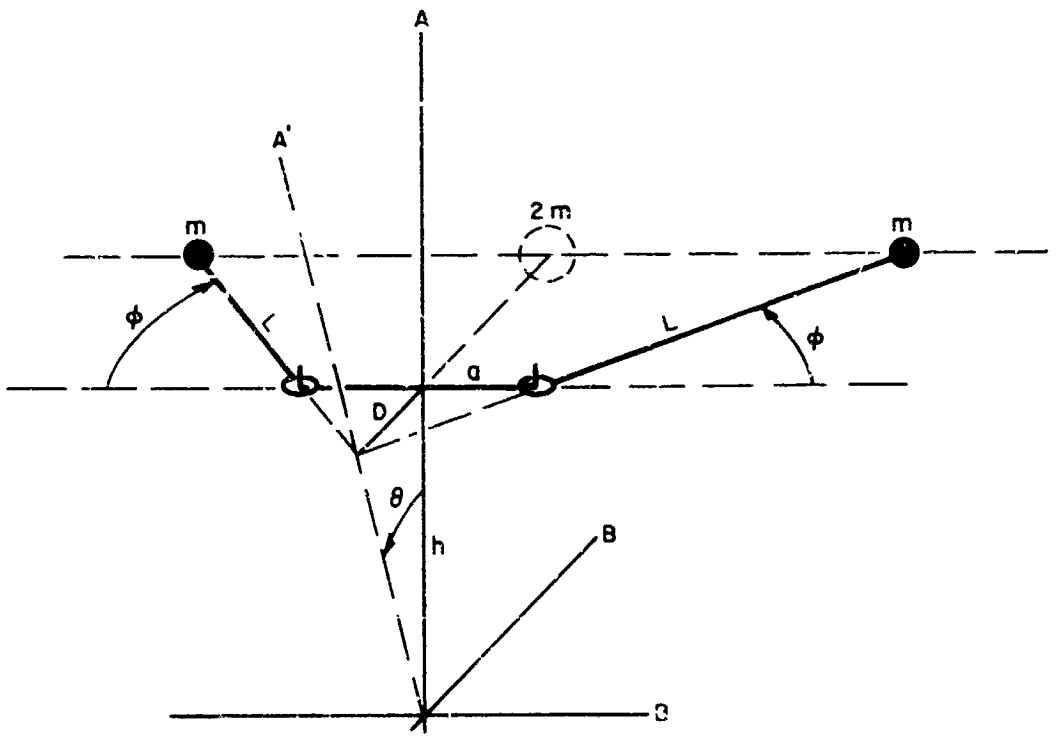

FIG. 14. Spin Axis, A', Displaced from Spin Axis, A.

The dynamic unbalance, Θ, resulting from a mass located at a distance, d_1, along the axis and d_2, off the desired principal axis, A, is given approximately by

$$\tan 2\Theta \doteq 2\frac{\text{mass}\cdot d_1 \cdot d_2}{A-B}$$

If the angle is small, the factors 2 can be dropped. In terms of the symbols above, the relation is:

$$\tan\Theta \doteq \frac{2mhL\sin\varphi}{A-B}$$

The distance, d, in Fig. 14 is used to relate the angles φ and θ as follows:

$$h\tan\Theta = a\tan\varphi$$

The formula for $\cos\varphi$ in terms of design parameters only, follows:

$$\cos\varphi = \frac{(A-B)a}{2mh^2L}$$

For design purposes this can be considered as a "stability criterion" in which the parameters must be selected such that S is comfortably greater than one.

Mercury-Ring Damper

In the early experimental work, a mercury damper was tried. It was expected (1) to have a resonant property, and (2) to provide a balanced configuration in the equilibrium state. A circular channel for fluid was carefully located concentrically with the symmetry axis of the simulator. The channel cross section was rectangular, wide radially, but narrow in the other dimension. Sufficient fluid was used to form a complete ring around the axis of the simulator when it was spinning and "sleeping." It may be seen that in this condition, there should be no unbalance; so an unbalance problem such as with the mercury drop is overcome.

A probable design criterion for this type of damper was pointed out in Ref. 3. Models of the fluid damper were tried and found to be very effective. Exhaustive tests, however, were not conducted primarily because a mechanical damper was preferred for the S-6 satellite.

S-6 SATELLITE NUTATION DAMPER DEVELOPMENT

EXTENDED MODEL EXPERIMENTS

Tuning Confirmation

A confirmation of the tuning condition was one of the first steps taken toward the development of a nutation damper specifically designed for the S-6 satellite. Simple, spherical pendulums were studied first. Later, a parallel investigation of compound pendulums was made, followed by extended work on controlled planar pendulums.

In an early tuning experiment with the small-model simulator, two pendulums, each of different length were prepared, one being 4.25 inches and the other 6.75 inches. The pendulum hinge pins were placed diametrically opposed, each located at 0.5 inch from the simulator axis and 1.75 inches above the c. g. of the test vehicle. The pendulums were not constrained by the hinges to swing in a plane normal to the symmetry axis, but could swing in any direction as spherical pendulums. The pendulum-bob weights were adjusted so that the simulator was balanced when spinning in steady state (or sleeping) with both pendulums in place. In addition, two fixed weights were prepared so that when either pendulum was removed, the weight would act as a balance for the other pendulum.

Simple nutation damping tests were made with this equipment, using the steel scale and stopwatch method, described on page 22. First, a single pendulum of one length was installed on the simulator, and many tests were made at each of several values of the moment of inertia ratio, A/B. The second pendulum was then similarly tested alone, and finally both pendulums together were tested. The c. g. was kept at the pivot point for all settings.

The results of these tests are shown in Fig. 15, 16, and 17. It may be noted that the damping effectiveness is not given in the usual way, by a damping coefficient which is the constant factor in the exponent of a negative exponential expression. This is intentional since there is definite experimental indication that the nutation does not decay smoothly as in such a simple expression, and this presentation serves to emphasize this point. Figures 15 and 16 show a dip (or increase) in damping very close to the resonance point predicted by the formula. Although the standard deviation of measurement is fairly high, these dips appear to be real and significant. Figure 17 shows the expected broadening of the resonance region when the two pendulums, tuned for slightly different configurations, are used together.

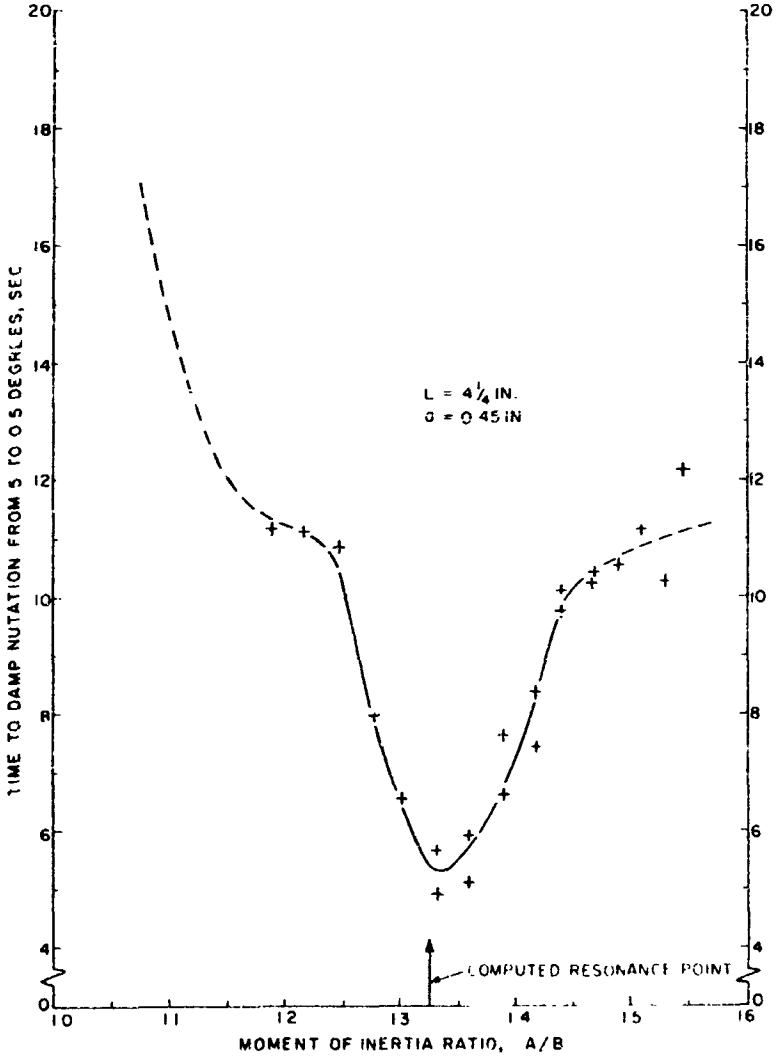

FIG. 15. Nutation Damping Record of Single Spherical Pendulum.

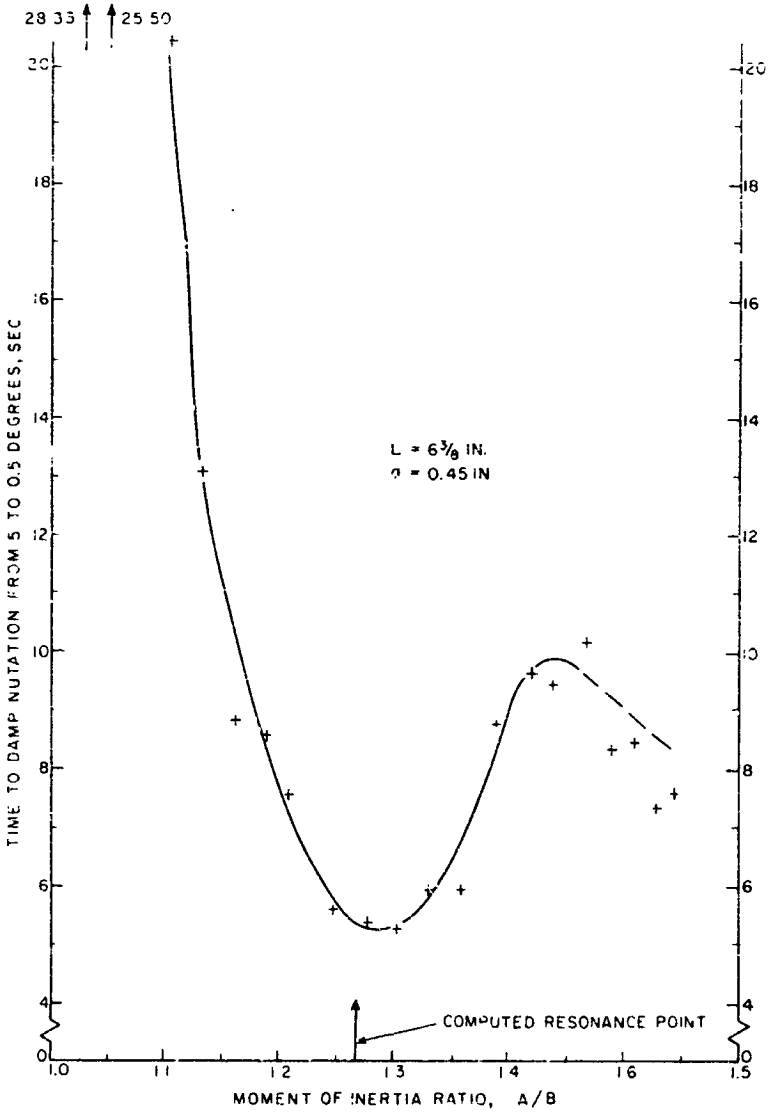

FIG. 16. Single Simple Pendulum Nutation Damping.

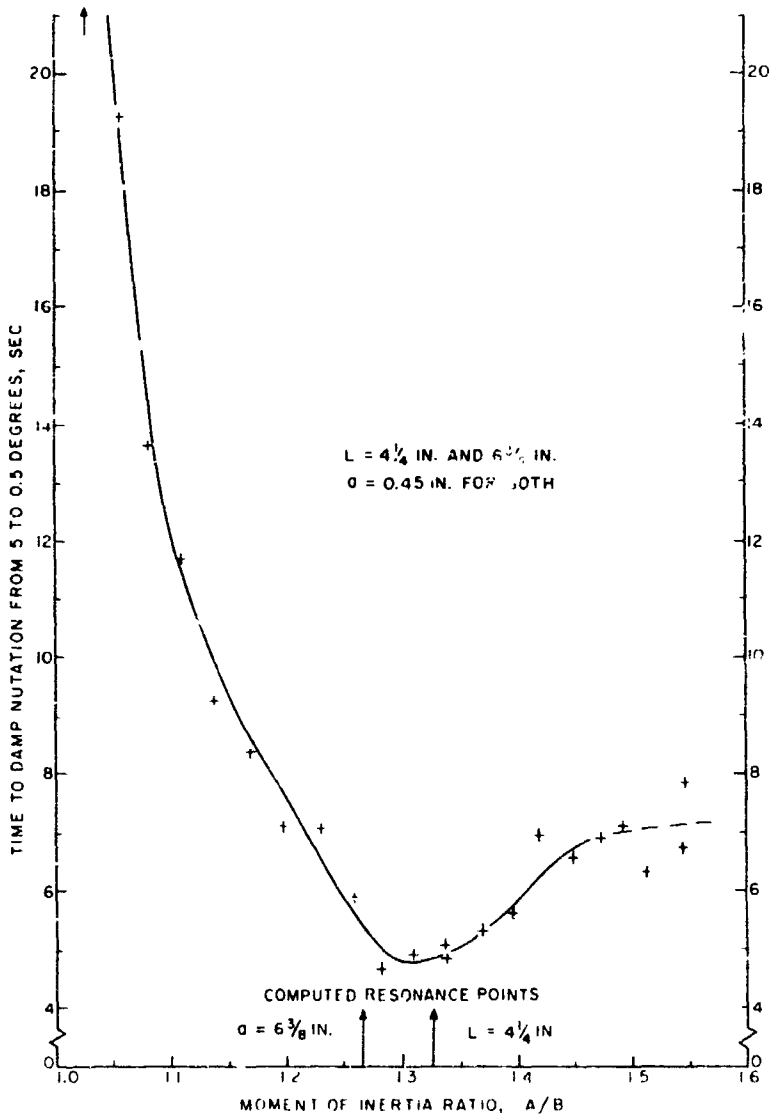

FIG. 17. Nutation Damping Record of Two Spherical Pendulums.

This experimental confirmation of a significant tuning effect made it appear advisable to investigate the use of compound pendulums. It was expected that the ratio of moments of inertia, A/B, for the S-6 satellite would be fairly close to unity, for example, 1.1 to 1.2, requiring a low-frequency pendulum. In addition, it was desirable to locate a damper inside of the satellite sphere where space was limited. Since both space and low pendulum-frequency were simultaneously determining factors, the effectiveness of compound pendulums was worth investigating.

Compound Pendulums

An ideally thin circular ring (or short hollow cylinder), rotating as a wheel about its hub, has a radius of gyration equal to the radius of the ring. This ring has a larger radius of gyration than any other body within the same maximum dimension. Let such a ring be the bob of a planar pendulum whose pivotal axis is normal to the plane of the ring and some distance outside of the ring (assume a weightless supporting arm). If the pivotal axis is now moved in successive steps toward the center of the ring, the pendulum period will first decrease to a minimum value, then increase rapidly to infinity as the pivot approaches the center of the ring. The period is minimum when the pivot is at the edge of the ring and in this position the period is the same as that of a simple pendulum, the length of which equals the diameter of the ring. The maximum dimension of this pendulum, that is, from the pivot to the far edge of the ring-shaped bob, decreases until the pivot reaches the near edge of the ring. Thereafter the size of the pendulum, namely the diameter of the ring, remains the same as the pivot moves toward the ring center. It is therefore theoretically possible to make a pendulum having any period in any desired size.

With this design principle in mind, compound pendulums were made in the form of rings of copper wire. The pivot point within a ring was provided by a hole in a diametral brass strip into which the pin in the simulator could fit loosely. Figure 18 shows an early model of a compound pendulum prepared in this way.

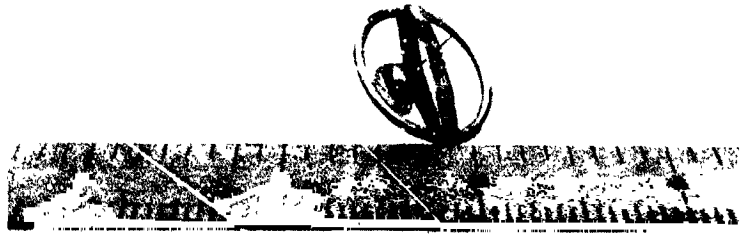

FIG. 18. Compound Pendulum.

The nutation-damping effectiveness of the compound pendulums tested was found to be less than that of simple pendulums of comparable weight and natural period. In particular, when the distance from the pendulum c. g. to the pivot point was much smaller than the radius of gyration, the nutation damping was very poor. Special attention was given to the hinges (or pivots) to insure that at the same time, there would be a minimum of "play" and very low friction. Only when the pivot was near the edge of the ring did the nutation damping compare well with the simple pendulums tested previously. Little or no space could be saved under these conditions, so work on compound pendulums was put aside, and development of basically simple pendulums was pursued.

Simple Pendulum Tests With Hinge Friction

The hinges (or pivots), made for the simple pendulums, were rather crude in the earlier tests. They did not constrain pendulum motion to one plane in the simulator, and the motion was like that of a spherical pendulum. Hinge damping torque was not controlled, although it was kept fairly low. Therefore, following the work with compound pendulums, a series of tests was undertaken with small-model simulators in which hinge designs were varied. The essential results of these tests are shown in Fig. 19.

As before, with each different pendulum configuration, the moment of inertia ratio was varied, and the time taken for nutation to damp by a factor of 10 (that is, from 5 to 0.5 degrees) was noted. The c. g. was kept very close to the center of the universal bearing in all runs; also for these tests, the pendulum length, L, pivot offset, a, height, h, and the bob mass, m, were kept essentially constant.

The hinges for the first two tests were made with 0.016-inch steel wire for the hingepins, and thin (approximately 0.014-inch) brass sheet with 0.018-inch-diameter holes served for the pendulum bearings. A spherical pendulum used a single bearing, whereas a planar pendulum had two bearings spaced one-half inch apart. Measurement of hinge friction for these pendulums showed less than 0.5% critical damping in the gravity of the earth, or about 0.45% critical damping in the simulator rotating at 8 rps.

In comparing the results of these first two tests with those of the earlier tests (Fig. 15), it was first noted that the nutation-damping effectiveness was much greater in the earlier tests. Some of this greater effectiveness is attributed to the differences in pendulum size and location; however, a large part of it certainly was due to reduced hinge friction in the later tests.

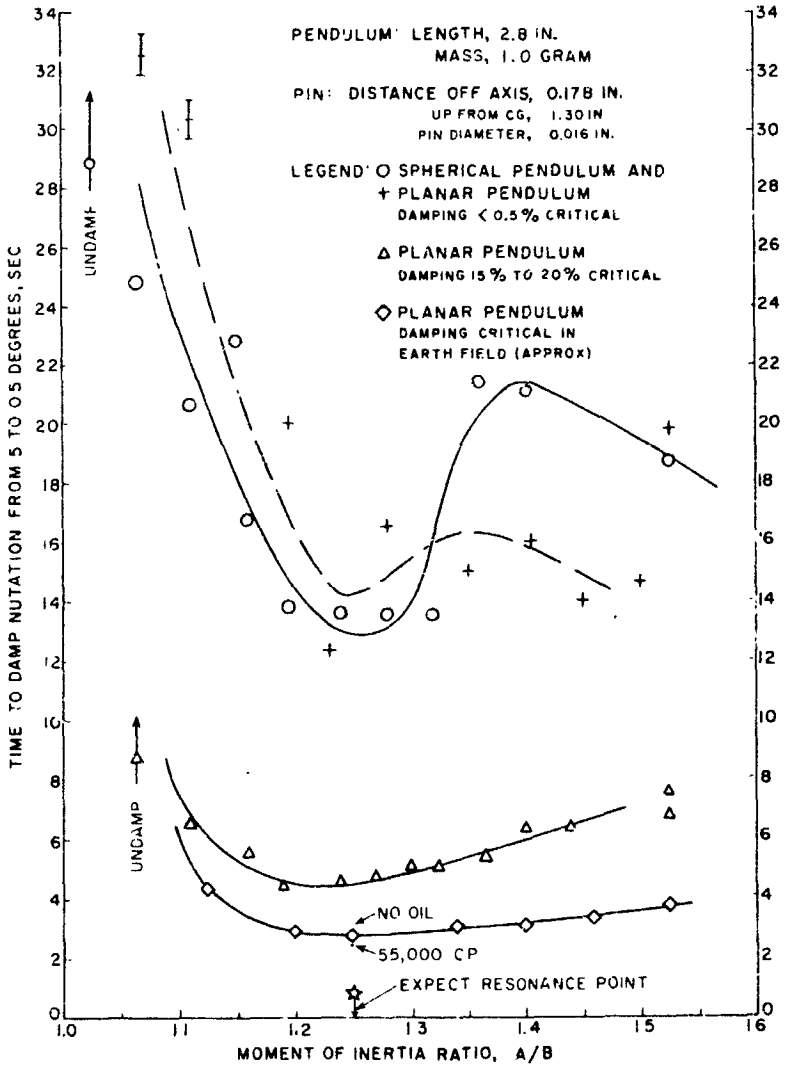

FIG. 19. Nutation Damping Records of Pendulum Hinge-Friction Variations.

Probably of equal significance is the observation that the dip at resonance was much less pronounced in all planar pendulum tests than in the earlier spherical pendulum tests. Indeed, the one spherical pendulum run (Fig. 19) showed this pronounced resonance feature. Although this fact is noted, no real use was made of it in the S-6 satellite damper design because space within the satellite was limited.

Tests of hinge friction were made by holding the pivot pin horizontally and swinging the pendulum in the gravity field. When friction is low, it is fairly easy to determine the hinge-damping coefficient as well as the natural frequency, or effective length of the pendulum. However,

when friction is high enough so that there are only two or three measurable swings, or when the pendulum damping is critical or greater in the gravity field of the earth, the determination of these pendulum parameters is more difficult. The special methods and formulas used in each case are discussed in Appendix A.

The data in the lower pair of curves in Fig. 19, were obtained after hinge friction was introduced by causing a spring, fastened to the pendulum, to press on the hinge pin. By adjusting the spring pressure, the amount of friction could be controlled, and the approximate amounts of hinge damping shown on the graph were obtained. Note that the initial step, producing about 15% of critical damping (in the spinning simulator), gave the greatest effect. However, the friction introduced in this way was mostly of the coulomb type, not strongly dependent on velocity and with significant static or starting torque. The static friction was particularly undesirable since with it, the pendulums would not, in general, come to rest in their diametrically opposed and balanced positions after the nutation was damped out. The steady state configuration, then, was unbalanced so that rotation was displaced somewhat from the symmetry axis. Nevertheless, if it is realized that this conditions exists, nutation damping tests can be made with reasonable reliability.

Finally, hinges better-designed to produce viscous friction were made. The hinge pin was made of the smoothly ground shank of a 0.094 inch drill. The pendulum bearing was made of a brass tube (or sleeve) approximately one-half inch long, drilled and reamed smoothly on the inside so that it fitted the pin with a radial clearance of about 0.0005 inch. These two parts were assembled carefully with a viscous lubricant in a manner to prevent bubbles from developing in the bearing space. The viscosity of the lubricant was used to control the hinge-damping coefficient.

At first, commonly available hydrocarbon oils were used as the lubricant. (Greases produce excessive static friction, undoubtedly, because they are somewhat crystalline in nature.) Then silicone oil, specifically "Dow Corning 200 Fluid," available in a variety of viscosities, was obtained. The viscosities varied by factors of about ten, from 100 to 100,000 centistokes.[6] Intermediate values are easily obtained by mixing the fluids. Even at the highest viscosities, this oil appears to retain Newtonian fluid flow properties. The formula used for estimating the required viscosity, and the method for testing viscosity of the mixed fluid are given in Appendix B.

[6]Since the specific gravity, ρ, of this fluid is 0.98 (approx.), the specific viscosity in centipoise (cp) is almost the same as the kinematic viscosity in centistokes (cs) by which it is specified. η(poise) = $\rho\nu$(stokes).

Results from nutation-damping tests showed this new pendulum to be very effective. Both minimum hinge-friction obtained with very light oil, and high hinge-friction obtained with 55,000-centistoke fluid that produced greater than critical hinge-damping gave characteristic nutation-damping times of about 3 seconds.

The shortest nutation-damping time was observed when the hinge friction was adjusted to give a little less than critical damping in the acceleration field of the spinning simulator model. The average time to damp nutations by a factor of 10 (from 5 to 0.5 degrees) was about 0.75 second, or about six turns of the simulator. This point is shown near the bottom center of Fig. 19.

The behavior of these planar pendulums, with almost pure viscous hinge-friction, showed such high effectiveness and reliability, and appeared to confirm the theory sufficiently well that design work on the full-scale damper for the S-6 satellite was begun.

DYNAMICAL THEORY

The theoretical study of the dynamical system to find analytical expressions for the rate of nutation damping proved to be quite involved. Approximate relations were derived by W. R. Haseltine (Ref. 4) in an analysis of the simulator with one, two, and four planar pendulums, and these relations were borne out, at least quantitatively, by both the small-model experiments and the tests on the full-scale S-6 satellite prototype.

The simulator and four planar-pendulum dampers are considered to be coupled oscillators by Haseltine. In this case, two diametrically opposed pendulums (of the four) are fixed, leaving two similarly placed pendulums free to oscillate. There are no applied outside forces or torques such as those caused by gravity. However, there are frictional torques about the hinge pins which couple the pendulums to the main body, and, of course, there are the coupling reaction forces at the pins. The torques consist of pure viscous friction of the type $\tau_i = -k\dot{\varphi}_i$, where φ_i are the pendulum angular positions relative to the simulator.

The kinetic energy is then given by

$$2T = A\omega_x^2 + B(\omega_y^2 + \omega_z^2) + m\sum(\dot{r}_i)^2 - \frac{m^2}{M^*}\left(\sum \dot{r}_i\right)^2$$

where

A = polar moment of inertia of the basic simulator

B = transverse moment of inertia of the basic simulator

ω_x, ω_y, ω_z = (in order) polar and transverse components of angular velocity of the simulator

m = mass of one damper pendulum-bob

M_* = M + 4m and M = mass of the simulator without any of the four pendulums

r_i = vector positions of the damper masses in an inertial coordinate system, $\dot{r}_i$ being the time derivatives

The r_i are, of course, functions of the variable pendulum angles, φ_i. The Euler-Lagrange relations are used to write the equations of motion in terms of the generalized coordinates, ω_x, ω_y, ω_z, φ_1, and φ_2, and first-time derivatives of each.

These differential equations are linearized by assuming:

1. Angular displacements are small;
2. Angular velocities of the pendulums and cross angular velocity of the main body are small compared to angular velocity about the spin, or symmetry axis;
3. Changes in spin rate are also small compared to the spin;
4. Moments of inertia, contributed by the damper masses, and those masses themselves are small compared to the corresponding quantities for the main body.

The five linearized differential equations (for two pendulums) are reduced to four by eliminating the variable part of the polar spin. The dependent variables are, then, the two components of cross spin-rate, ω_y and ω_z, and the two pendulum angles, φ_1 and φ_2. The independent variable is time, actually transformed to average spin turns, s. Solutions in the form of exponentials, $\theta = A \exp(-\alpha + ib)2\pi s$, are tried and the results are investigated, mainly, for the largest values of α, the damping factors. Here, as usual when the exponent is imaginary with α and b real, α is the damping coefficient and b is the main frequency indicator; also $i \equiv \sqrt{-1}$.

Basic Design Relations

The essential conclusions of the analysis can be briefly stated. In the case of the two-pendulum damper, when the damping rate, α, is not at maximum and the hinge friction is higher than optimum, the following expression holds:

$$\alpha = \frac{\beta(\delta + 1)^3}{(\rho - \delta^2)^2 + K^2\delta^2}$$

This expression is given entirely in terms of the dimensionless parameters used by Haseltine. In terms of real design parameters, his parameters are:

$$\beta = \frac{mh^2}{B} = \frac{m^2h^2L^2}{BI}$$

$$\delta = \frac{A}{B} - 1$$

$$\rho = \frac{a}{L} = \frac{maL}{I}$$

$$K = \frac{k}{mL^2\Omega} = \frac{k}{I\Omega}$$

To repeat some symbols, the real physical parameters are:

A = polar moment of inertia of the main body

B = transverse moment of inertia of the main body

I = moment of inertia of a pendulum about its hinge axis

L = length of the pendulum from the hinge axis to the c. g.

a = distance of the pendulum hinge pin from the symmetry axis of the main body

h = height of the pendulum c. g. above the c. g. of the main body

k = pendulum-hinge coefficient of friction in "torque = $-k\dot{\varphi}$"

m = mass of the pendulum b-b

Ω = polar spin of the main body in radians/second

It is seen that a maximum value, or a resonance condition, occurs when

$$\rho = \delta^2$$

When K is small, a better approximation for the damping factor is simply

$$\alpha = \frac{K}{4}$$

These two expressions represent α poorly at a value of K which satisfies both of them (Fig. 20). However, a good first approximation to optimum hinge friction is obtained by their simultaneous solution. Under the resonance condition this solution is

$$K = 2\sqrt{\frac{\beta(\delta + 1)^3}{\delta}} \quad .$$

Both the analogue solutions of the equations and the experimental data show that the actual optimum K lies somewhat higher than that given by this formula.

Referring again to the tuning criterion, $\rho = \delta^2$, in dimensional design parameters, this is

$$\frac{a}{L} = \left[\left(\frac{A}{B}\right) - 1\right]^2$$

or

$$L = \frac{a}{\left[\left(\frac{A}{B}\right) - 1\right]^2}$$

for the simple pendulum, as given on page 25. It is to be noted that this resonance formula was found in a less rigorous fashion and given previously in Ref. 3. There, incidently, a modifying term is included which indicates that a longer arm would be resonant, and therefore more effective at larger nutation angles, θ,

$$L = \frac{a + \left(\frac{Ah}{B}\right)\theta}{\left[\left(\frac{A}{B}\right) - 1\right]^2} \quad .$$

From this, one might suspect that two pendulums of unequal length would be more effective in damping out large nutation amplitudes than two equal pendulums would be. However, no conclusive test for this added term was made. For the record, a brief derivation of this formula is given in Appendix C.

It is instructive to look again, also, at the expression for the nutation-damping coefficient, α, simplified for the resonance condition, but this time in terms of the dimensional parameters, that is,

$$\alpha = \frac{\Omega A^3}{(A - B)B^3} \frac{(mhL)^2}{k} \quad .$$

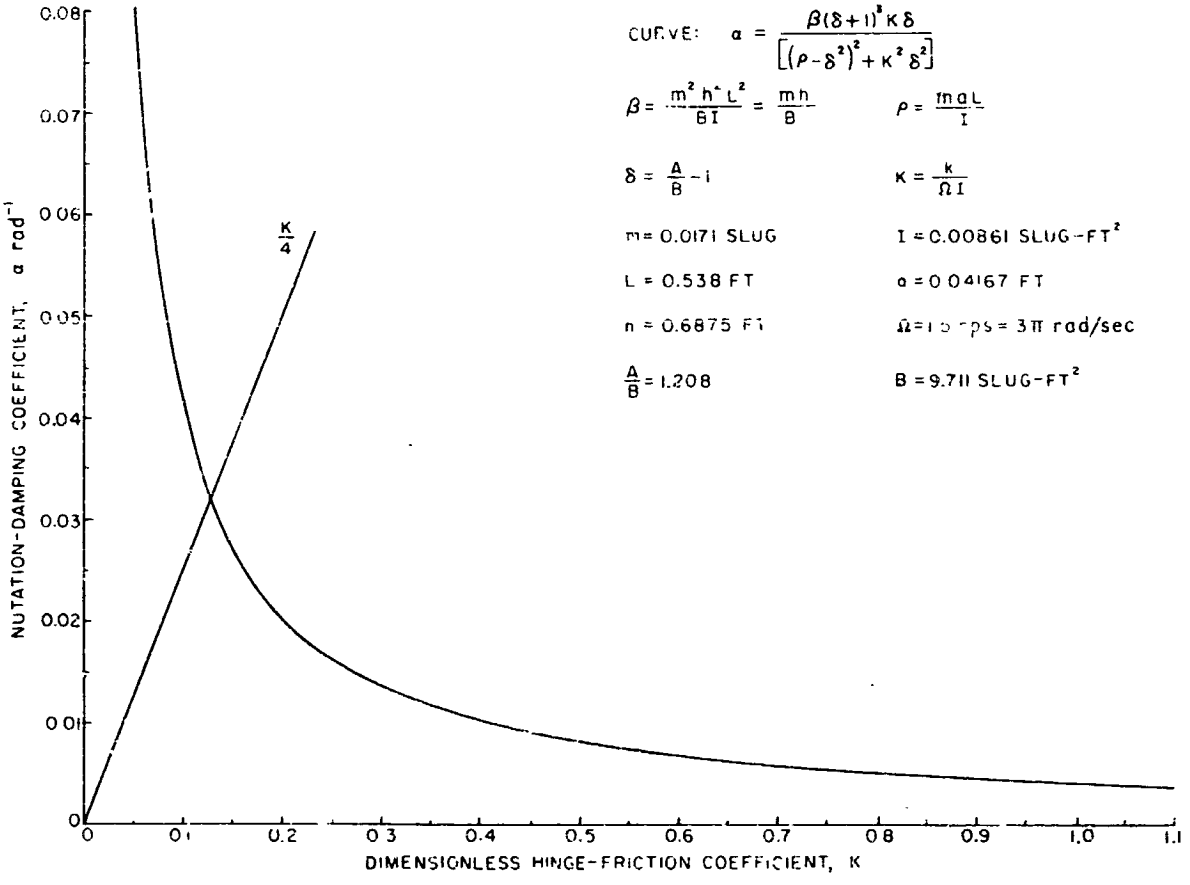

FIG. 20. Nutation Damping Dependence on Pendulum Hinge-Friction (Theoretical).

Here the parameters have been grouped according to whether they pertain to the basic satellite or to the pendulum nutation-damper mechanism. Note that α increases as the square of the pendulum mass, length, and distance from the satellite c. g. However, these cannot be increased without limit, for the stability criterion must be observed.

Placement Accuracy and Vehicle Balance

Good dynamic balance of an entire space vehicle is very important since an uncaged pendulum nutation damper can increase any unbalance. It has been stressed that the intended spin axis must be the axis of maximum moment of inertia. Basically, a dynamic balancing process consists of rearranging mass until this inertial axis and the symmetry or desired spin axis coincide.

The vehicle will normally be balanced while the damper twin-pendulums are caged, that is, clamped in place along a straight line through the hinge axes. During vehicle flight in steady state, the pendulums will be free to swing and will align themselves radially from the final spin axis. If this spin axis falls on the line connecting the pendulum hinges, the initial balance of the vehicle will be undisturbed. If, however, the damper is placed poorly in the vehicle, or if the vehicle is improperly balanced so that the principal dynamic axis falls a short distance away from the line between the hinges, the pendulums will not be aligned in steady state and will therefore create additional unbalance. From this, a basis for the placement tolerance in the vehicle fabrication and assembly can be obtained. The allowable residual equilibrium unbalance will be determined by the vehicle mission and the instruments within the vehicle.

The following relations were derived for two types of fabrication problems, that is, balance, and damper placement. First, assume that a perfectly made damper unit is precisely placed on the symmetry axis of a vehicle. However, a dynamic balancing error displaces the principal axis of inertia an angle, Θ_u, away from the symmetry axis. The uncaged damper will then increase the unbalance to Θ_R as follows:

$$\Theta_R \pm \left(\frac{1}{1-\gamma}\right)\Theta_u$$

where

$$\gamma = \frac{2mh^2L}{a(A-B)}$$

and all other symbols are as before.

Next, assume that the satellite with damper installed and caged is balanced perfectly such that the principal inertial axis is coincident with the symmetry axis, but that the damper is placed a distance, d, off the symmetry axis in a directional normal to the line between the hinges. The uncaged damper will then create a dynamic unbalance, Θ_d, as follows:

$$\Theta_d \pm -\left(\frac{\gamma}{1-\gamma}\right)\frac{d}{h}.$$

Summary of Design Criteria

To recapitulate, the basic design criteria for the twin-pendulum damper are as follows:

1. Stability criterion is expressed by the quantity, S, which must be greater than unity:

$$S = \frac{(A - B)a}{2mh^2L} > 1$$

2. A measure of nutation damping effectiveness is

$$\alpha = \frac{\beta(\delta + 1)^3 K\delta}{(\rho - \delta^2)^2 + K^2\delta^2}$$

or, at resonance

where $\rho = \delta^2$,

$$\alpha_R = \frac{\beta(\delta + 1)^3}{K\delta}$$

3. The resonance condition is

$$\rho = \delta^2$$

or

$$\frac{mLa}{I} = \left(\frac{A - B}{B}\right)^2$$

4. A good estimate for optimum hinge friction is

$$K \doteq \left[2\sqrt{\frac{\beta(\delta + 1)^3}{\delta}}\right] 1,2$$

However, final adjustment by experiment should be made.

5. Placement tolerance: Ideally, the vehicle axis of maximum moment of inertia intersects the midpoint of the line between the pendulum damper hinge pins. (1) Small displacement of the axis along this line changes nothing but the resonance situation. (2) Small displacement of the axis away from the line changes the equilibrium position of the pendulums, thereby creating an increasing unbalance.

For displacement owing to dynamic unbalance, Θ_u, total unbalance is

$$\Theta_R = \left(\frac{1}{1 - \gamma}\right) \Theta_u$$

For displacement caused by damper offset, d, resulting unbalance is

$$\Theta_d = \left(\frac{\gamma}{1 - \gamma}\right) \frac{d}{h}$$

where

$$\gamma = \frac{2mh^2L}{a(A - B)}$$

FULL-SCALE DYNAMICAL SIMULATOR

To facilitate the design and fabrication of a nutation damper for the S-6 satellite, two different full-scale simulators were used. The first one, the laboratory model (Fig. 21), was made similar in design to the table models; the transverse moment of inertia could be varied easily. The second simulator consisted of the No. 4 prototype model of the S-6 satellite sphere, modified so that it could be mounted at its center on the universal bearing. The areas of primary interest in the construction of a full-scale simulator are the bearing, the alignment and balancing methods, and the nutation damping tests.

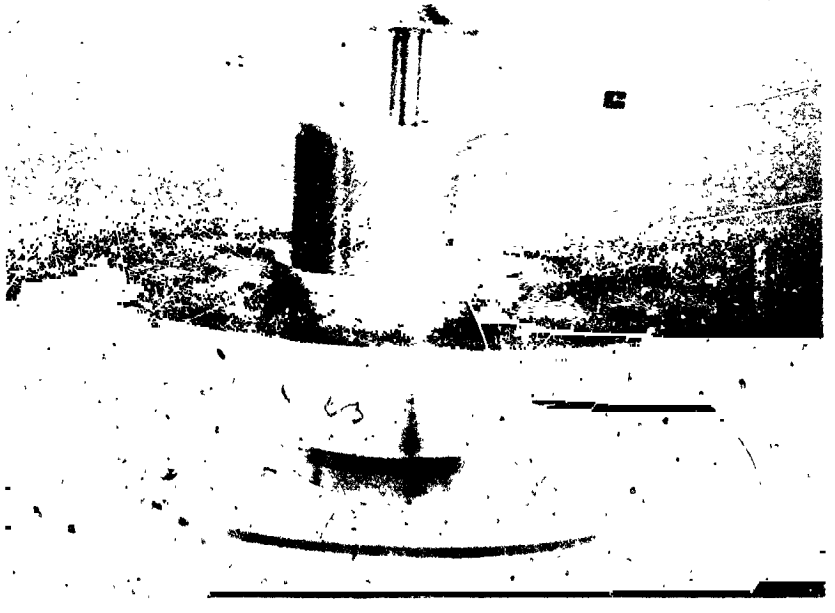

FIG. 21. Full-Scale Dynamical Simulator.

Bearing

Since ball bearings were adequate for the small-model simulators, it seemed reasonable at least to try them for the full-scale model. The universal bearing was made from Chevrolet "pick-up" U-joint parts. So that one yoke of the joint would be stationary, it was screwed onto the top of a stiff upright supporting post. The shank of the other yoke was modified to accept the spin axis bearings (Fig. 22).

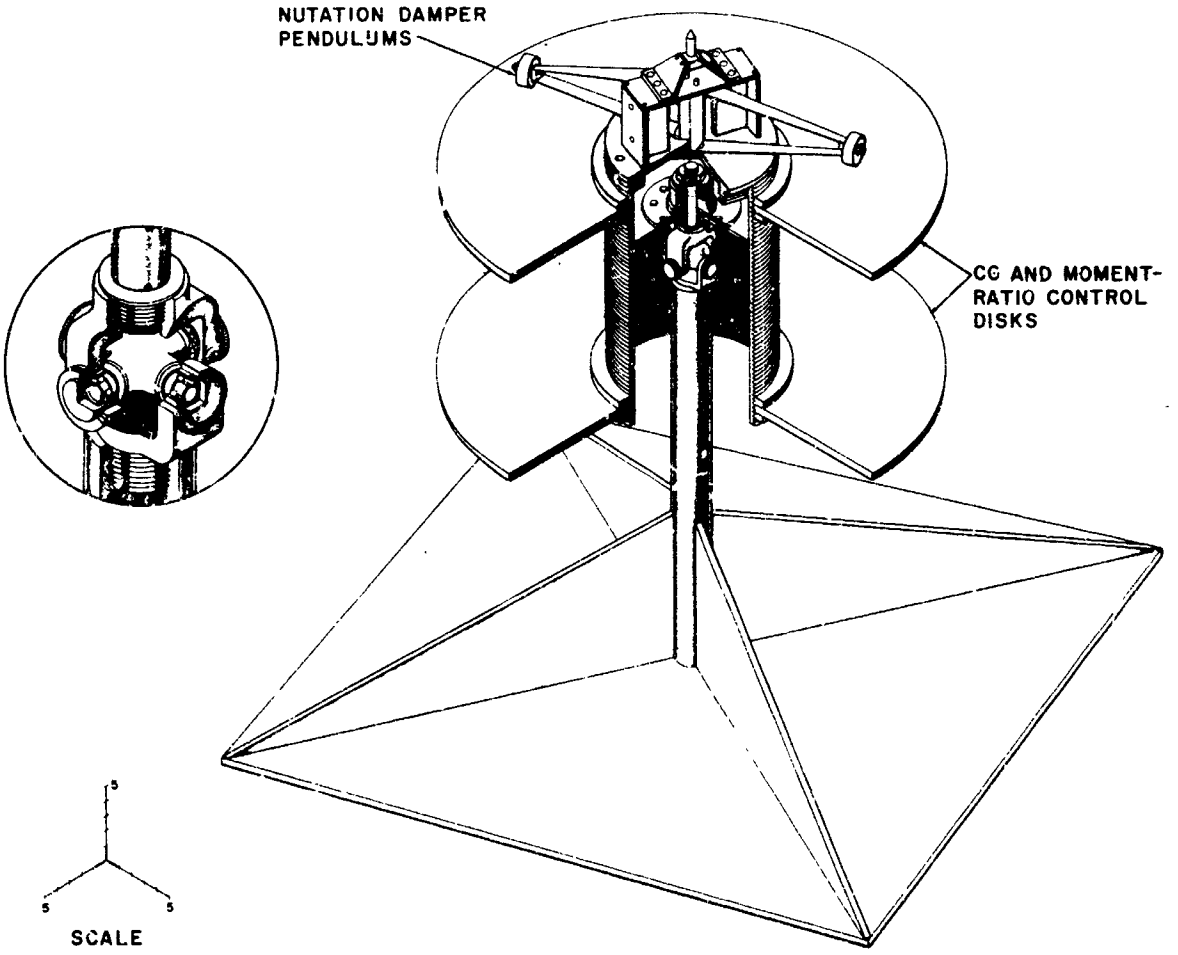

FIG. 22. Upper Yoke and Bearings of the Dynamical Simulator.

To minimize friction, the grease-packed roller bearings of the U-joint cross were replaced by standard sized New Departure (N. D.) Q0L01 ball bearings. The spin bearings were N. D. Q0L05 ball bearings. All bearings were the angular contact type intended to take full axial loads. All bearings were of instrument quality and were lubricated with a low viscosity high-pressure oil. All bearing mounts were designed to permit application of an axial preload, although only a slight

preload was given. Light axial-loads were expected in the cross bearings and a unidirectional axial-load in the spin bearings. Lateral bearing play could not be allowed, and the light preload insured this condition.

Alignment

To simulate the space environment of a rotating sphere, on which there are essentially no outside torques, the c. g. of the body must be at the center of all rotation. In a three-axis gimbal then, all three axes must intersect at a single point, namely at the center of the cross-piece in the U-joint.

The bearing seats on the U-joint cross were carefully machined so that the two transverse bearing axes very nearly intersected, and at very close to 90 degrees. This alignment was checked by measurements on the controlling surfaces with a Mann comparator of near 1-micron accuracy. The problem remaining was to align the third or polar spin-axis with the intersection of these transverse bearing axes.

The initial machining of the spin-bearing seats in the upper yoke did not put the spin axis close enough to the transverse bearing axis in this yoke. To provide adjustment, an eccentric sleeve was made to fit (thumb press) over the reduced yoke spindle. The outside diameter of the sleeve fitted closely (thumb press) the bore of the spin bearings. By rotating the eccentric sleeve, the spin axis was adjusted until it intersected the transverse axis in the yoke. Adjustment of the other transverse axis was made by moving the entire yoke with respect to the cross by means of the preload adjustment caps in this upper yoke. It should be noted that the position of the lower (or fixed) yoke with regard to the cross did not affect the alignment or balance problems.

Measurement of alignment was made with the aid of two dial indicators contacting surfaces on the cross. The assembly was held by the spin bearings, permitting rotation about the spin axis. One indicator was used to insure normal attitude of the cross, while the other measured the cross displacement from the spin axis.

This bearing alignment procedure was usually satisfactory. However, the final test came after the full-scale model was mounted, balanced, and spun. Any residual misalignment was evidenced by a slow precession always to one side. It was then necessary to note the direction of error (90 degrees from the direction of precession) and to remove the universal assembly to make a correction.

In the first full-scale simulator (laboratory model), the intrinsic symmetry was sufficiently good that alignment of the assembly about the spin-bearing axis was no problem, and very little adjustment to

balance was needed for initial testing. However, when a simulated battery pack was mounted on the disks, balance became a problem. Later when the No. 4, S-6 prototype was used, both mounting and considerable balance adjustments were necessary.

To provide access to the center of the prototype satellite sphere through its base, the dummy lower mass spectrometer (Fig. 1) was removed, and the attachment fitting (also shown in Fig. 1) was cut out farther, leaving in the sphere an 8-inch diameter hole. An adapter unit (Fig. 23) for mounting the universal bearing was fabricated, consisting of (1) a three-tiered disk, which bolted onto the bottom of the main instrument platform in the satellite, and (2) a threaded cylinder, which could be screwed up or down within the disk. In the top of the cylinder, the spin bearings were mounted and by screwing the cylinder up or down, the c. g. of the prototype could be brought to the level of the cross bearing axes.

A jig for holding dial indicators was made to align the adapter unit to the satellite shell. The spin-bearing shaft, to which this jig was bolted, was fixed in the satellite but did not spin with it, and the shaft protruded through and above the adapter unit. An indicator, contacting the top of the main joint (Fig. 1) of the lower hemisphere of the satellite (with the upper hemisphere removed), indicated tilt of the spin axes which was corrected by means of shims between the adapter and the main instrument platform. Indicators on the outsides of both the main joint (large ring) and the attachment fitting (small bottom ring) of the satellite showed offset error and also checked tilt. Slightly oversize bolt holes in the adapter disk permitted the desired lateral corrections to be made.

Balance

As stated previously, the laboratory model required little attention for alignment and balance because it was inherently symmetrical in design. The prototype satellite, however, required careful static and dynamic balance and with the single universal bearing mount, definitions of these quantities are in order. For static balance, the c. g. of a satellite must coincide with the intersection of the three perpendicular bearing axes. For dynamic balance in addition to static balance, the axis of greatest moment of inertia must be made to coincide with the symmetry axis of the satellite. It should be noted that for all balancing operations, the nutation damper was clamped (or caged) in neutral position.

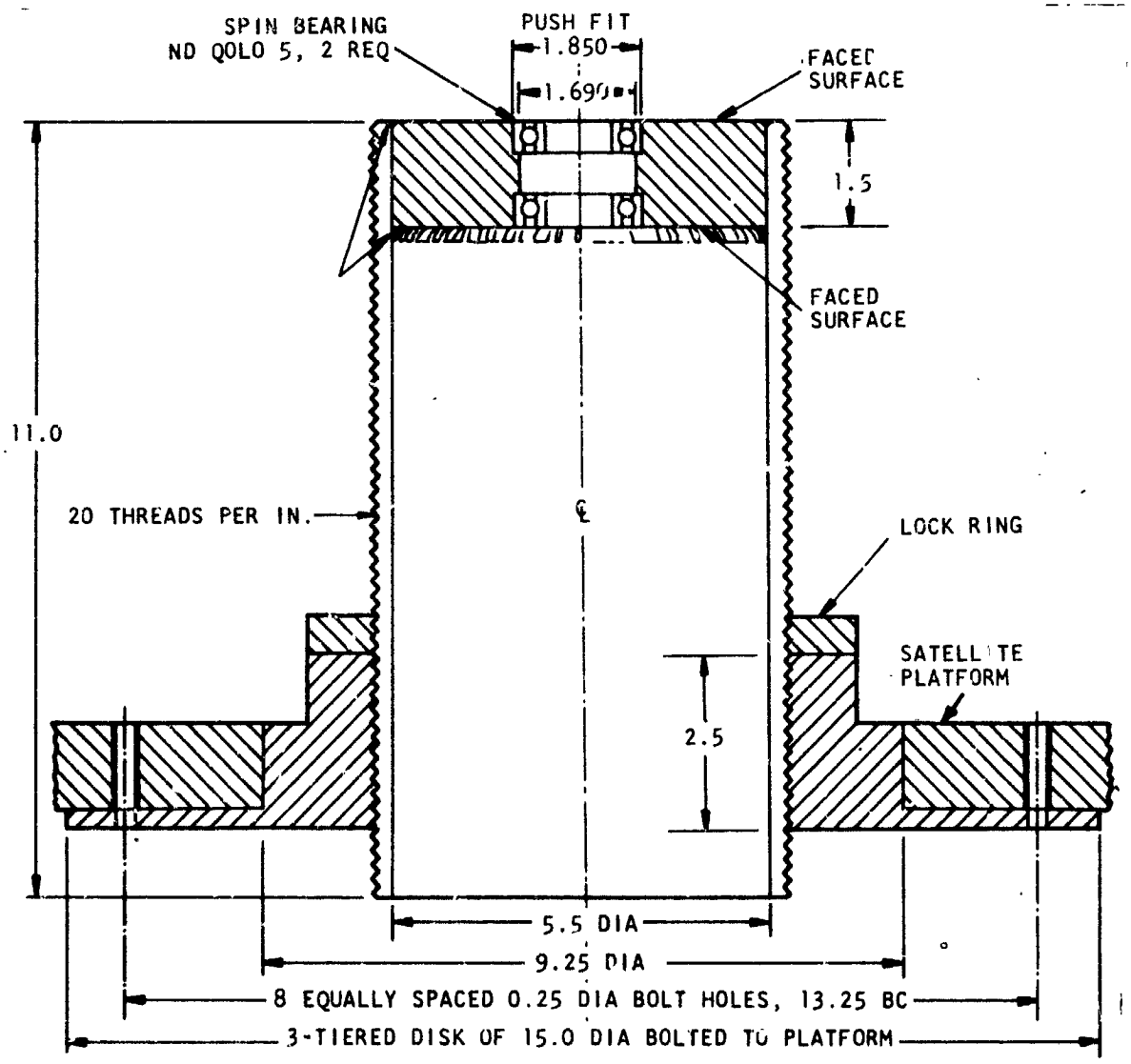

FIG. 23. Universal Bearing, Satellite Adapter Unit.

Probably the best static balance of a simulator can be made with the simulator spinning. A strain gage (or other) pickup on one side of the supporting post will indicate the location and amount of unbalance in the horizontal plane containing the transverse axes. To detect vertical displacement of the c. g., the spinning simulator can be tipped so that the spin axis is not vertical. The moment caused by gravity will then give the vehicle a circular precession, the direction of which is easily detected.

No doubt because the bearings were of high quality, very good static balance was obtained when the simulator was not spinning. Both horizontal and vertical unbalance were observed equally well by tipping the supporting post until it was horizontal. With the spin axis weighted to maintain a horizontal position, the heavy side of the simulator was allowed to settle downward. This heavy side was then rotated 90 degrees and balanced there with calibrated weights on the opposite side (Fig. 24). The corresponding moments about the vertical and horizontal axes were computed, and equivalent moments were established by permanently mounted weights inside the sphere, and by screwing the adapter cylinder up or down.

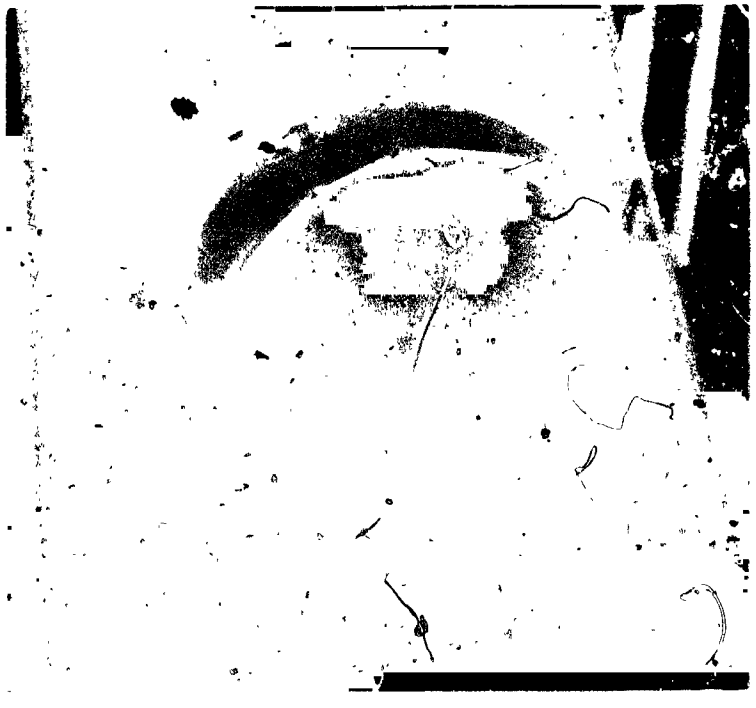

FIG. 24. Arrangement for Satellite Balancing.

In some cases, good horizontal static balance was obtained with the simulator in a normal upright position. The calibrated weights were merely placed on the closure ring of the satellite until balance was found.

The dynamic balance procedure was more interesting. First, to facilitate adjustment, three special weights on threaded shafts were installed inside the prototype satellite at almost equally spaced positions close to the skin (Fig. 25). These positions were indicated for weights in Goddard Space Flight Center Drawing No. J-S6-74.

After this preparation, the sphere was spun to 3 or 4 rps which provided good gyroscopic stiffness, that is, angular momentum, and a small amount of friction was applied manually near the spin axis. This soon removed all nutational vibration and the spin was stabilized about the axis of greatest moment of inertia. With the sphere in this condition of spin, a piece of soft chalk, held lightly on the sphere near the symmetry axis, drew a good circle, the center of which was the actual spin axis at that time. The sphere was then stopped and a divider or compass was used to find the center of the marked circle. The extent and direction to which this center was displaced from the symmetry axis of the sphere was a measure of the dynamic unbalance to be corrected by moving the internal weights.

For the initial trials when unbalance was large, chalk marks on the metal sphere surface were satisfactory. For final adjustment, however, a circular disk of drawing paper was glued to the sphere, concentric with the symmetry axis, so that precise circles could be drawn on the paper with a sharp pencil. Unbalance indication of less than one-sixteenth of an inch, or about 10 minutes of angle was easily measured by this method.

FIG. 25. Weight for Dynamic Balancing Adjustment.

Moments of Inertia

After alignment and balance were completed, weight and moments of inertia were measured on the prototype satellite. Although this prototype contained a full complement of dummy instruments and batteries, in an arrangement expected to be final, many and extensive changes were subsequently made before the satellite was finally launched.

For the moment of inertia measurements, a 0.125-inch-diameter steel wire about 8 feet long was attached to the sphere to form a torsion pendulum. The wire was calibrated with the steel disks made for the full-scale laboratory model simulator. The period with the 370-pound prototype was about 30 seconds.

It was anticipated that the satellite, complete with dummy instruments and batteries, would not have equal transverse moments of inertia. Therefore, more than one transverse measurement was needed, and it was desirable to ascertain a minimum number. In one determination, measurements were made at four orientation angles: 0, 45, 90, and 135 degrees from the + y axis, and a fifth angle at 180 degrees to check the 0-degree reading (Fig. 26). This method appeared

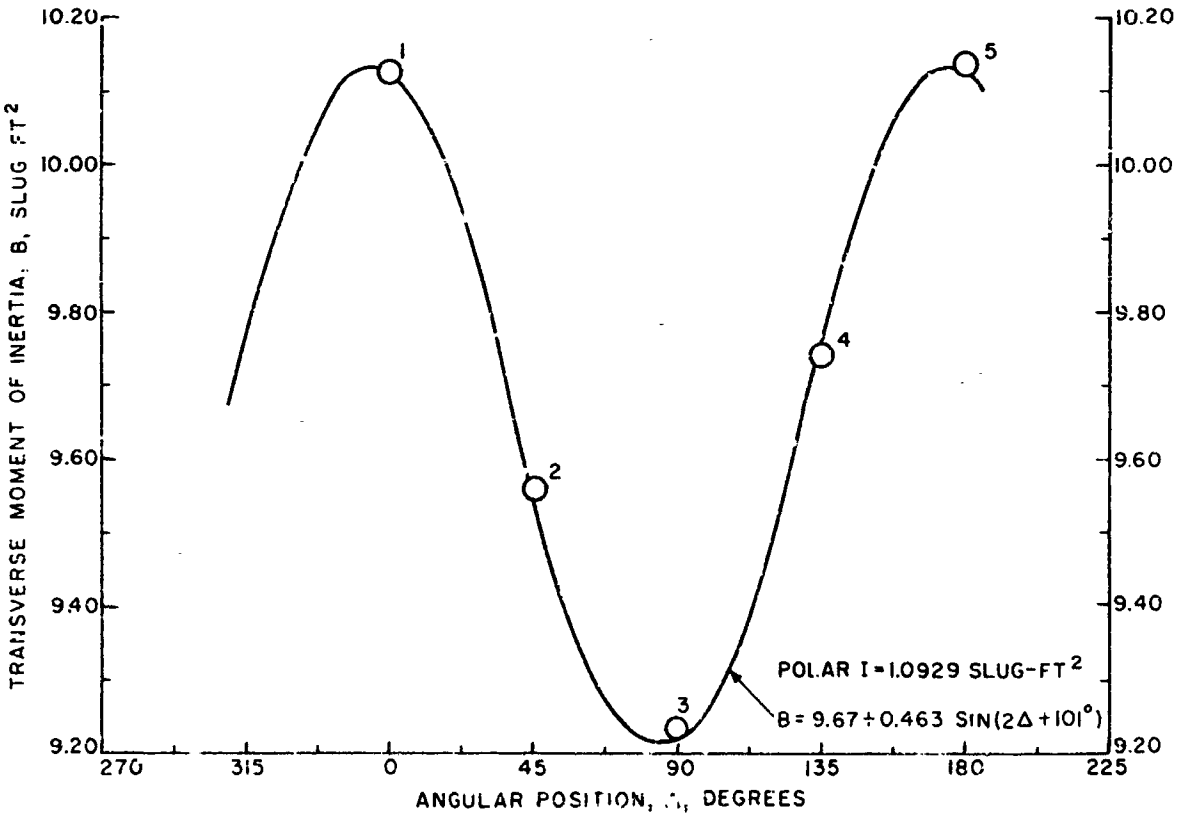

FIG. 26. Variation of Transverse Moment of Inertia with Angular Position.

to determine the maximum and minimum values very well when a sine curve was faired in by eye. A least squares fitting technique[7] was also suggested. This technique actually does not take very long to perform since there are so few data points.

One might obtain sufficient information from only three measurements separated by 45 degrees, however, this would provide no redundancy to reduce experimental error. Further, if the three points should happen to be like 2, 3, and 4 in Fig. 26, there would be danger of misinterpretation wherein the existence of points 1 and 5 might not be realized.

FULL-SCALE NUTATION-DAMPING TESTS

Damping Measurements

Measurements of nutation damping on the No. 4 prototype of the S-6 satellite were made both visually and photographically. The visual measurement was much faster, of course, and actually gave a good measure of the essential results. The procedure setup, shown by Fig. 27 and 28, shows the scale, grid, and clock arrangement near the model.

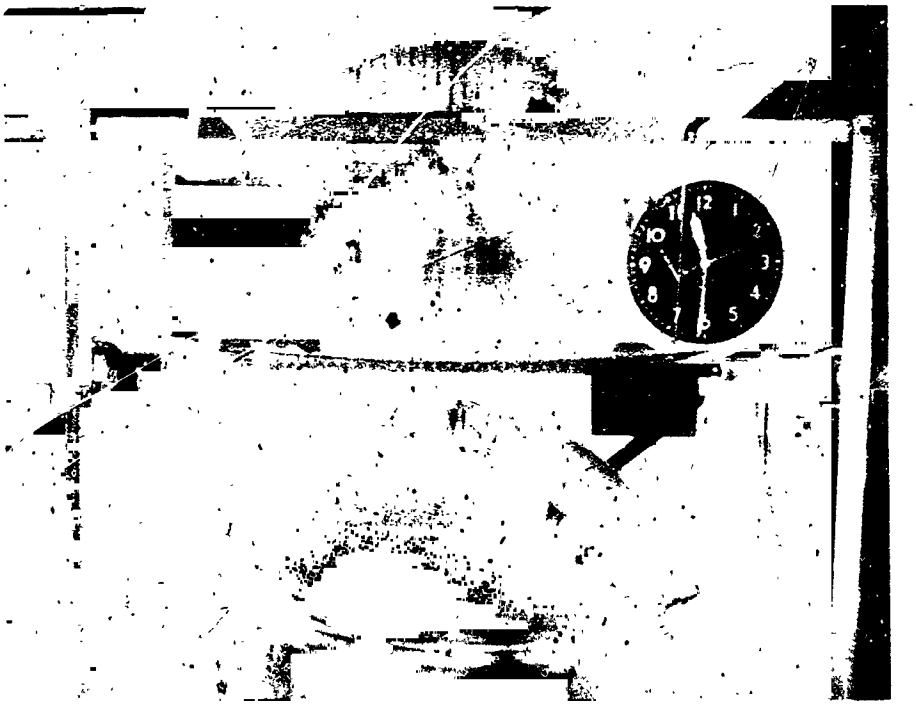

FIG. 27. S-6 No. 4 Prototype Dynamical Test Setup.

[7] U. S. Naval Ordnance Test Station. Dynamic Stability Investigation for the NASA Atmospheric Structure Satellite (S-6), Progress Report VIII, by H. L. Newkirk. China Lake, Calif., NOTS, 3 August 1961. (NOTS Technical Note 4065-155.

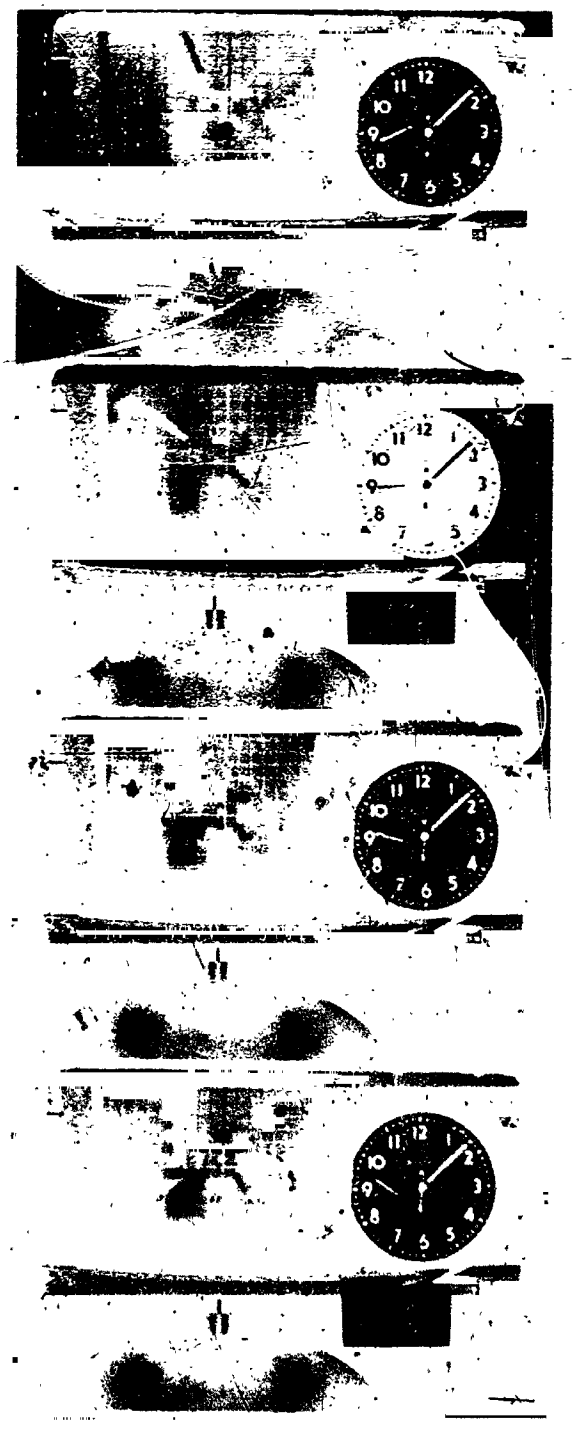

FIG. 28. Nutation-Damping Test Metric Film.

The satellite was accelerated to the desired spin by means of a 0.5-inch electric drill turning a 6-inch-diameter rubber-tired cart wheel. This function normally required two men, one to operate the drill and one to steady the satellite by placing his gloved hand on the smooth spindle, indicating the top of of the symmetry axis. Maximum speeds were from 2.5 to 3 rps.

It was difficult to induce a significant amount of nutation with a single blow on the spindle of the satellite. However, any desired amplitude could be obtained easily by manually pushing the spindle sideways in a spiral motion. The action appeared to be like that of producing a fast circular precession by application of a force normal to the instantaneous motion of the spindle, and then removing the force suddenly.

When the nutating satellite was viewed from the side at a point about level with the top, the spindle appeared to oscillate back and forth in front of the linear scale, shown in Fig. 28. (An observer should be as far away as possible to minimize parallax error.) Good visual measurements of nutation-damping can be made in this way if a stop-watch is started when the oscillation of the spindle is at an amplitude of, say, 4 inches and stopped at 0.5 inch. This method corresponds to a half-angle of about 6 degrees maximum and a factor of 8 decrease. To determine spin at these low rates, the turns of the vehicle can be counted, and the time for ten or twenty turns can be measured accurately enough with the stopwatch. A sample of data obtained in this way is shown in Table 2.

TABLE 2. Sample Visual Nutation-Damper Measurements: NASA S-6 Satellite, No. 4 Prototype With Pendulum-Damping Units

t_N[a]	t_{10}[b]	t_{20}[b]	t_N[a]	t_{10}[b]	t_{20}[b]
A. Unit B (1,635-cp fluid in hinge; k^c = 0.017 lb-ft-sec/radian)					
7.19	....	.....	6.14	....	.....
....	4.10	8.20	5.64	....	.....
6.84	....	.....	....	6.65	13.38
6.89	....	.....	6.20	....	.....
7.58	....	.....	5.10	....	.....
....	4.68	9.30	5.20	....	.....
7.62	....	.....	4.90	....	.....
....	5.16	10.30	....	7.75	15.52
7.60	....	.....	6.00	....	.....
6.95	....	.....	5.65	....	.....
....	5.78	11.46	4.90	....	.....
7.10	....	.....	4.46	....	.....
6.18	....	.....	4.92	....	.....
6.70	....	.....	....	9.60	19.25
7.47	....	.....	....	....	.....
B. Unit C (3,280-cp fluid in hinge; k^c = 0.032 lb-ft-sec/radian)					
3.50	....	.....	5.35	....	.....
....	3.68	7.54	5.80	....	.....
4.96	....	.....	....	6.16	12.29
3.80	....	.....	5.87	....	.....
4.35	....	.....	6.00	....	.....
....	4.27	.....	6.80	....	.....
4.55	....	.....	6.28	....	.....
....	5.04	10.07	6.80	....	.....
5.75	....	.....	....	7.15	14.23
5.22	....	.....	8.12	....	.....
4.75	....	.....	8.25	....	.....
5.20	....	.....	8.40	....	.....
....	5.75	11.45	8.40	8.45	16.95
5.05	....	.....	....	....	.....

[a] t_N is time (sec) for nutation to change from 5.6 to 0.7 degrees, or $\theta_0/\theta = 8.0$. At nutation angles larger than about 5 degrees, the pendulum arms hit their stops.

[b] t_{10} and t_{20} are times (sec) for 10 and 20 turns of the satellite.

[c] [illegible]

With these data obtained visually, a figure can be determined for the damping coefficient, α, in the expression

$$\frac{\theta}{\theta_o} = \exp -\alpha(2\pi st)$$

where st is the number of turns between the nutation amplitudes θ_o and θ. Many such measurements can be made quickly, and delay for film developing and reading is not necessary.

More detailed information could be obtained with the aid of a moving picture camera, located as far as possible to the side of the satellite. The camera lens was located at the level of the spindle, which protruded from the top of the satellite. For visual measurements, the eye was located at the same level. The camera was set for 32 frames per second, producing ten or more pictures per turn of the satellite. It is desirable, however, to reduce the camera shutter-angle in order to get short exposure time. A 45-degree shutter angle at 32 frames per second gives a 1/256-second exposure, producing less than a 3-degree smear if the simulator is turning at 2 rps. Black and white high-speed film was used with photo floodlights in this setup.

In Fig. 28, the top of the satellite is viewed through a grid by means of an overhead mirror. The grid, made of cords accurately spaced one inch apart, was placed about 2 inches above the spindle of the satellite so that parallax would be minimized. The tip of the spindle was 20 inches above the center of the universal bearing. The clock in the picture was standard until a fourth hand that made one turn per second was added, making it fairly easy to interpolate to one-twentieth of a second. With this kind of setup, both the orientation and the magnitude of the nutation angle can be measured as functions of time.

Much of the data, obtained by the visual method from tests of the final production dampers on the final configuration of the S-6 satellite No. 4 prototype, are shown in Table 3. The test data are arranged in order of increasing hinge-fluid viscosity. This is reflected in the values for dimensional hinge-friction coefficient, k. Two corresponding non-dimensional coefficients, K, that depend on spin are given. A graph of these data is shown in Fig. 29; the damping coefficient, α, is plotted against the non-dimensional hinge-damping coefficient, K. The theoretical curves, K/4, and the inverse relation are included.

At least the general form of these relations is supported by the data. In particular, it is interesting to note (Tables 2 and 3) how the nutation damping varies with spin in any one test. For low values of k, damping time, t, decreases for lower spin, and fewer turns are required for the given decrement. At higher values of k, the damping time actually increases at lower spin, although the number of turns to damp does not change much with spin.

TABLE 3. Consolidated Nutation-Damping Data, NASA S-6 Satellite No. 4. Prototype with Pendulum-Damper Units

Test date 1962	Damper unit	Hinge fluid viscosity, η, cp	Hinge-friction coefficient			Spin, s, rps	Damping time, [b] t, sec	Turns to damp, st	Nutation-damping coefficient, α radians^{-1}
			k[a]	K, s = 2.0 rps	K, s = 1.5 rps				
27 Feb	C'	(c)	0.00008	0.00074	0.00098	2.34	48.8	114.1	0.0029
						1.66	40.35	66.91	0.0049
						1.29	56.	72.26	0.0046
27 Feb	E	100	0.0011	0.010	0.0135	1.89	29.	54.72	0.0063
						2.33	28.	65.41	0.0051
						1.97	26.	51.23	0.0065
						1.5	28.	42.	0.0078
27 Feb	F	1,000	0.009	0.083	0.111	2.27	10.0	22.7	0.0146
						1.70	9.7	16.52	0.0200
6 Mar	B	1,735	0.017	0.16	0.21	2.44	7.0	17.07	0.0194
						1.74	7.0	12.22	0.0271
						1.49	6.2	9.28	0.0359
7 Mar	E	1,735	0.0106 (0.0137)	0.11	0.15	2.48	9.0	22.30	0.0148
						1.92	7.6	14.97	0.0221
						1.54	7.7	11.89	0.0278
7 Mar	F	1,735	0.0116 (0.0135)	0.12	0.16	2.56	9.5	24.52	0.0135
						2.09	8.0	16.75	0.0198
						1.56	8.3	12.93	0.0256
						1.35	8.0	10.82	0.0306
12 Mar	E	2,400	0.023 (0.020)	0.20	0.27	2.44	6.2	15.16	0.0218
						1.92	5.24	10.06	0.0329
						1.67	4.95	8.27	0.0400
12 Mar	F	2,400	0.020 (0.019)	0.18	0.24	2.27	7.73	17.56	0.0188
						1.98	7.33	14.53	0.0228
						1.75	7.09	12.40	0.0267
						1.46	5.63	8.27	0.0400
						1.26	5.07	6.39	0.0518
6 Mar	C'	3,280	0.032	0.30	0.39	2.65	4.0	10.61	0.0312
						1.98	4.55	9.04	0.0366
						1.63	5.8	9.44	0.0351
						1.41	6.5	9.13	0.0363
28 Feb	B	12,500	0.106	0.98	1.31	2.69	11.90	32.03	0.0103
						2.31	12.8	29.56	0.0120
						1.70	17.0	28.96	0.0114

[a] The units for hinge-friction coefficient, k, are lb-ft-sec/radian. When only one value is given, k is the same for both pendulums of the pair.

[b] The nutation amplitude changed by a factor of 8 from about 5.6 to 0.7 degrees in all cases. At nutation angles larger than about 5 degrees, the pendulums reached their maximum swing and hit the stops.

[c] The inner cylinder of the hinge assembly was removed to obtain minimum hinge friction.

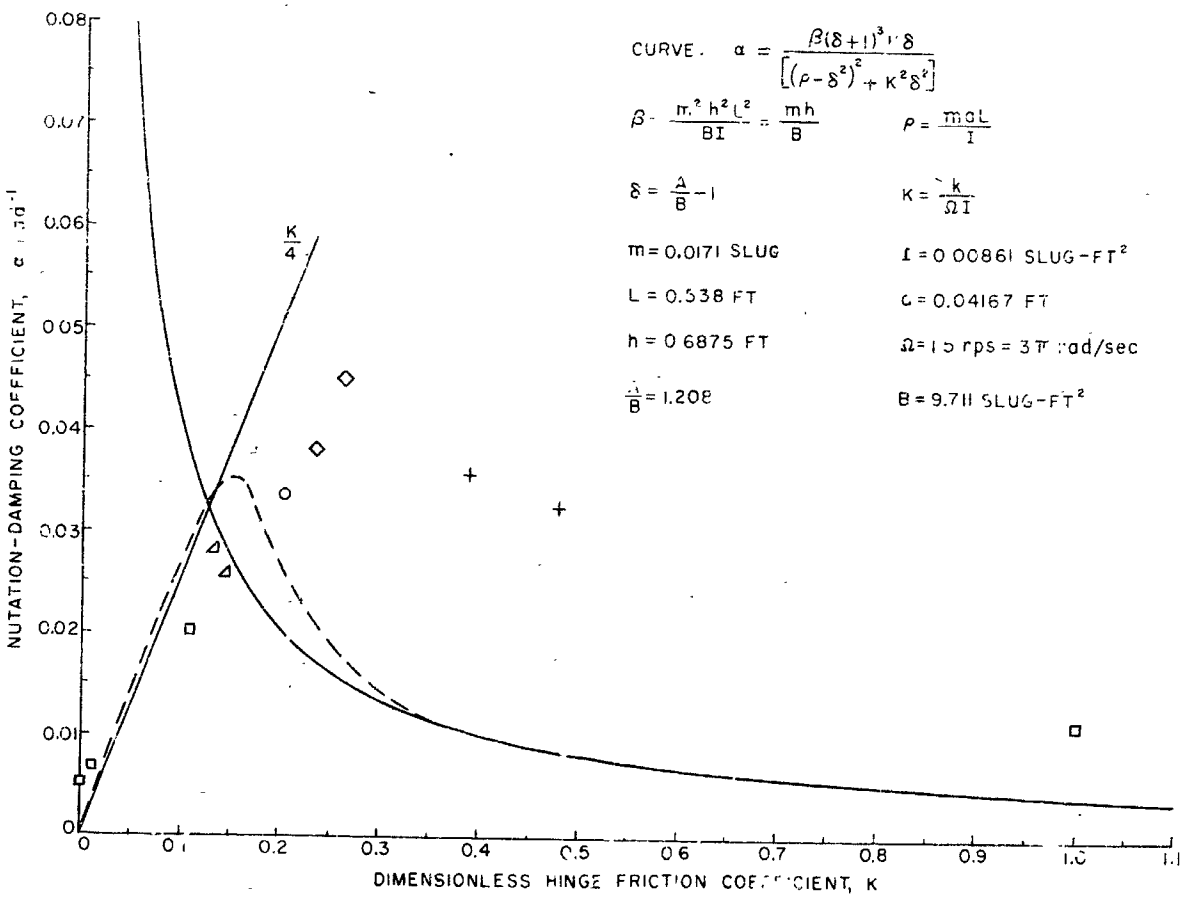

FIG. 29. Nutation-Damping Dependence on Pendulum Hinge-Friction; Theory and Data Compared.

Special Experiments

It is to be noted that two special experiments were made, the first on the effect of the wet battery fluid, and the second to determine air-damping.

Wet and Dry Batteries. The first experiment, a test for the nutation-damping effect of fluid in the battery pack, involved the most work. Spent Silvercel batteries of various sizes were obtained to make up the pack (as shown in NASA drawing No. J-S6-74). These batteries first were packed on the lower disk of the full-scale laboratory-model simulator and preliminary runs were made. Figure 30 shows this unit being swung for transverse moment of inertia. The nutation decay was not detectably different from that for the rigid body.

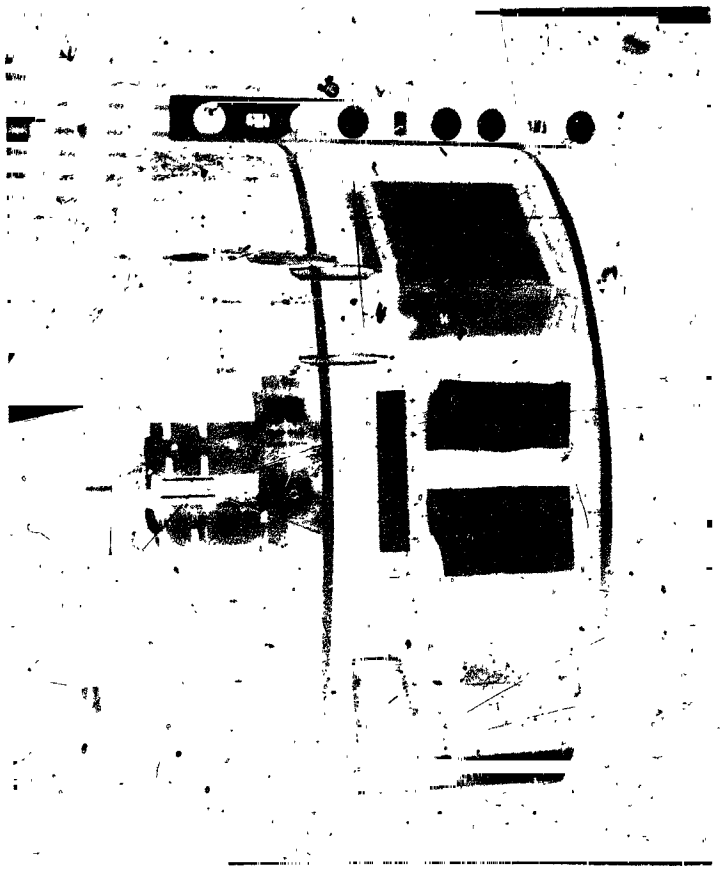

FIG. 30. Full-Scale Dynamical Simulator with Wet Battery Pack and Early Pendulum Damper Being Swung for Transverse Moment of Inertia.

As soon as the No. 4 prototype became available, the wet batteries were installed in the battery boxes (included with the prototype), and damping tests were made. These batteries were then replaced by dummy batteries made of wood and loaded with lead slugs and lead shot. As initially received, however, the lead in these dummies was loose and required potting with a plastic compound before they could be used in the nutation-damping test. Again, no difference between the nutation damping with the wet batteries and with the dummy dry batteries was detected.

The conclusion was not that the wet batteries had no effect on nutation damping. Nevertheless, whatever effect existed was well below that of the pendulums with minimum hinge-friction, which damped nutation by a factor of 8 in about 40 seconds. In comparison, for both the rigid body and the wet battery-loaded satellite, the same nutation decrease required about ten times as long, or over 5 minutes. During this time, spin changed by a significant percentage. It was concluded

that to determine the damping effect of the battery fluid, a much more elaborate experiment would have been needed. Air or fluid bearings and evacuated room environment might have been necessary, and, in particular, fast methods of changing from the wet to the dry condition with the required balancing would have been needed (or two identical models could have been used).

Air-Damping. The second experiment was performed to determine the effect of air on the nutation-damping tests. The No. 4 prototype was moved to the NOTS All-Weather Environmental Chamber for these tests. This chamber is a 12-foot square room in which pressure, temperature, and humidity can be controlled, and, particularly, changed rapidly to simulate aircraft climbs to high altitude and return. Observations were made inside the chamber with a GSAP electrically operated camera (50-foot magazine), and from outside the chamber with an Eastman "Special" camera (100-foot film roll), viewing the satellite through a window. To start nutations for the tests, the aid of a Navy jet-aircraft pilot, with pressure suit and oxygen equipment, was enlisted.

Two simulated ascents were made to a pressure altitude of about 60,000 feet, corresponding to one-tenth atmosphere of pressure. For one ascent the pendulum nutation-dampers were caged, and for the other ascent they were uncaged. One caged-damper start was recorded, and about eight uncaged-damper starts were made before spin became too low, making descent necessary in each case. These tests were made on 11 August 1961 and were followed immediately by control runs at standard 1-atmosphere pressure.

The intention was to make any adjustments in the procedure found necessary after inspection of the film and then to make additional ascents as necessary. However, the experiments were interrupted by rain storm damage to the pumping and refrigeration equipment of the chamber, and further testing (within a reasonable time) became impossible. Therefore, these were the only data obtained.

Again, it was felt that results were inconclusive because for the caged runs, it appeared that nutation damping was less at one-tenth of an atmosphere than it was at one atmosphere. In the uncaged runs, nutation damping was greater at one-tenth of an atmosphere. Spin deceleration was significantly less at one-tenth atmosphere. If nutation damping for the caged case had been less in thick air than in thin, one might justify it by reasoning that polar-spin deceleration from air should have been higher than the corresponding cross-spin deceleration. This effect would be much less pronounced for the uncaged case since time for each test was much shorter. This rationalization, however, was not given a chance.

It should be noted that there are a number of photographic records of tests made on the full-scale models which have not been thoroughly analyzed. After data sufficient for the development problem, had been obtained from a test, activity continued with the design or the production work. Analysis of detailed model-motion, in the hope of increasing basic understanding, was not done. A few of the better records may be so analyzed at a later date.

General Comment

It may be amply evident from the foregoing that highly accurate measurements of nutation damping were not attempted. For the S-6 satellite, the requirement was to damp out nutations "in the order of minutes." The effect of air drag at the surface of the earth would probably do this to the dynamic model even if the bearings were perfect. Instead, the attempt has been to make valid comparative tests. It is confidently felt that this type of testing permits the detection of any significant and perhaps even fairly small effects; it certainly allows sufficiently accurate selections of optimum design conditions for a pendulum nutation-damper which is effective in the order of seconds. It is apparent, therefore, that the use of the simplified experimental apparatus has been justified.

SUMMARY

From early experiments with small-model dampers, it was concluded that a pendulum-type nutation damper would be particularly advantageous for use in the NASA S-6 (Explorer 17) satellite that was subsequently launched in April 1963. Reported here are the experiments which confirmed the tuning condition, and, particularly, a new parameter relationship that was found, which controls a region of instability or undesirable performance. Further experimentation is reported which shows that (1) tuning is sharper for spherical- than for planar-pendulum dampers, (2) compound pendulums are not advantageous for obtaining compactness with tuning effectiveness, and (3) viscous hinge-friction is necessary for strong nutation damping. In particular, the best nutation damping was obtained when hinge friction was near critical pendulum damping for the centrifugal force field in which it operated. Approximate relations between the basic design parameters are given, based upon an associated theoretical study.

Full-scale dynamical testing is discussed which confirms the small-model experiments. In tests to determine the influence of (1) fluid in wet batteries used in the satellite, and (2) air-damping in the experiments, it was found that these effects were too small to be determined with the test setups used. The tested effects, however, were at least a factor of ten below the damping of the nutation damper when least effective, that is, with essentially zero hinge friction.

Damper environment in the satellite is stated in the Introduction, and a full list of BuWeps drawings is given for the full-scale damper design. In addition, some design considerations for the critical hinge, with provision for viscous friction, and for an uncaging device are discussed.

Appendix A

PENDULUM HINGE-FRICTION-COEFFICIENT MEASUREMENT TECHNIQUES

The properties of the nutation damper pendulums were most easily determined by swinging them in the gravity field of the earth. For this, Newton's law is written in the following form (small-angle approximation accepted):

$$I\ddot{\theta} + k\dot{\theta} + c\theta = 0$$

where

I = moment of inertia of the pendulum about its hinge axis

k = hinge-damping torque coefficient

c = the restoring moment coefficient

θ = angular displacement from the vertical

The coefficients I, k, and c are to be found.

First, note that

$$c = mgL$$

where

m = pendulum mass

L = distance from the hinge axis to the pendulum center of gravity

g = gravitational acceleration of the earth

These properties are most easily measured directly, using a balance and knife edge for m and L.

Note, also, that

$$I = m(L^2 + \rho^2)$$

where

ρ = radius of gyration of the pendulum about its center of gravity.

The solution of the differential equation is of the form

$$\theta = \sum A_i \exp(-\lambda_i t)$$

where

$$\lambda_{1,\,2} = \alpha \pm \sqrt{\alpha^2 - \beta^2}$$

and

$$\alpha = \frac{k}{2I}$$

$$\beta = \sqrt{\frac{c}{I}}$$

and for all $i > 2$,

$$A_i = 0$$

Three different kinds of motion are typified by the nature of the radical term in λ_i as follows:

Oscillatory	when	$\alpha < \beta$
Over damped	when	$\alpha > \beta$
Critically damped	when	$\alpha = \beta$

Each type of motion presents a different problem for finding the remaining coefficients I and k.

The determination of k is simplified greatly if I can be found first, by swinging the pendulum with the hinge friction reduced to a negligible value. This was easily done with the pendulum dampers by assembling the hinge with the ball bearings only, omitting the fixed inner cylinder of the viscous friction mechanism. The time, t_n, for a large number of swings, n, is then measured by means of a stopwatch, and I is computed as follows:

$$I = \frac{c}{\omega^2}$$

or

$$I = \frac{mgL}{4\pi^2} \left(\frac{t_n}{n}\right)^2$$

where ω is the frequency expressed in radians/second and is actually the quantity measured here. This is an approximation to

$$I = \frac{c}{2\omega^2} + \sqrt{\left(\frac{c}{2\omega^2}\right)^2 - \left(\frac{k}{2\omega^2}\right)^2}$$

for

$$k \longrightarrow 0.$$

Oscillatory Case

For the oscillatory case with a significant amount of hinge friction, the amplitudes of several successive swings of the pendulum are observed by letting the pendulum swing in front of a grid. Sufficiently good observation can be made visually since the frequency is not high; although continuously moving film photography would be used for better accuracy. The exact formula for the damping coefficient is

$$k = \frac{I\omega}{\pi n} \ln\left(\frac{\beta}{\omega} \frac{\theta_o}{\theta_n}\right)$$

where θ_o and θ_n are the amplitudes, respectively, of a selected initial swing and the n^{th} one thereafter. Here, ω contains the damping coefficient so that an iteration procedure is required for solution. However, even when the damping is so high that the amplitude decreases by a factor of 10 in as few as 3 or 4 swings, the effect on frequency is small, of the order of 1%. The following approximate formula can then be used:

$$k \doteq \frac{I\omega_o}{\pi n} \ln\left(\frac{\theta_o}{\theta_n}\right)$$

where

$$\omega_o \doteq \beta$$

is the frictionless, natural frequency in radians/second. Note that the time for these swings is not used since large percentage errors can be made in the stopwatch timing of the second or so required for so few swings.

These formulas are derived from the general solution for the oscillatory case with initial conditions θ_o and $\dot{\theta}_o$, namely:

$$\theta = C \exp(-\alpha t) \cos(\omega t - \phi)$$

where

$$C = \frac{1}{\omega}\left(\dot{\theta}_o^{\,2} + 2\alpha\dot{\theta}_o\theta_o + \beta^2\theta_o^{\,2}\right)^{1/2}$$

$$\phi = \cos^{-1}\frac{\theta_o}{C}$$

and

$$\omega = \sqrt{\beta^2 - \alpha^2}.$$

We let

$$t = 0$$

when

$$\dot{\theta} = 0$$

and later observations are made when

$$\cos(\omega t - \phi) = 1.$$

Over-Damped Case

For the over-damped case, the general solution can be written

$$\theta = A \exp-(\alpha-b)t - B \exp-(\alpha+b)t$$

where

$$A = \frac{1}{2b}\left[(\alpha+b)\theta_o + \dot{\theta}_o\right]$$

$$B = \frac{1}{2b}\left[(\alpha+b)\theta_o + \dot{\theta}_o\right]$$

and

$$b = \sqrt{\alpha^2 - \beta^2}$$

so that always $b < \alpha$.

The performance here was observed by using a General Radio Strobotac, flashing at a known, slow rate to illuminate the pendulum after it had been displaced from vertical and released. A multiple exposure picture was obtained during this time by means of a Polaroid-Land camera held open for a 1-second, or a bulb, exposure. The room light was subdued and points near the pendulum tip and hinge axis were prepared to give high-lights for measurement use. The vertical position of the pendulum was well spotted to provide a zero reference. The data obtained were pendulum angles from vertical and time interval between successive angles.

If the damping is much greater than critical, such that b is significant compared to α, curve-fitting or iterative methods for determining α are required. The deviation from a simple exponential is shown in the following form of the solution

$$\theta = \theta_o \exp^{(-\alpha t)}\left[\frac{\sinh(bt+\phi)}{\sinh\phi}\right]$$

where

$$\phi = \tanh^{-1}\left(\frac{b\theta_o}{\alpha\theta_o + \dot{\theta}_o}\right)$$

The ratio of hyperbolic sines in the square brackets can be much different from unity for significant values of b, even for rather small values of t. In fact, for finite t the bracket does not in general converge to unity as b approaches zero, that is, at critical damping.

Critical Damping

At critical damping the solution becomes

$$\theta = \theta_o \exp(-\alpha_c t) \left[1 + \left(\alpha_c + \frac{\dot{\theta}_o}{\theta_o} \right) t \right] .$$

It is seen that only if the pendulum is started at a particular downward speed, can this bracket be unity. If, as in the tests, the pendulum starts from rest ($\dot{\theta}_o = o$) and is photographed at intervals beginning, say, one-twentieth second later, this factor can be in the neighborhood of three by the time θ/θ_o is about 1/8. This emphasizes the need for the special data-reduction methods. However, the critical damping condition can be used to estimate high hinge-friction coefficient. If a small downward initial speed produces a single slight over-shoot, the hinge coefficient is approximately the critical value, namely:

$$\alpha_c = \beta$$

or

$$k_c = 2\sqrt{mgLI} .$$

Appendix B

HINGE-FLUID VISCOSITY SPECIFICATION AND MEASUREMENT

The basic definition of Newtonian fluid viscosity, η, is given by the formula

$$F = \frac{AV}{d} \eta$$

where F is the tangential force required to move a surface of area, A, at velocity, V, when separated from a similar surface by a distance, d, and when the intervening space is completely filled by the fluid. If the force is in dynes, the length in centimeters, and the time in seconds, the viscosity is in the units of poise (dyne second per centimeter^2). In common use is the unit, centipoise (or 0.01 poise).

The nutation-damper hinges have closely spaced concentric cylinders to provide the required viscous hinge-friction torque. In the dynamical equation, the magnitude of this torque is

$$\tau = k\dot{\phi}$$

where $\dot{\phi}$ is the angular velocity of the pendulum about its hinge pin and k is the friction coefficient, the design quantity specified. The problem is to determine the required corresponding fluid viscosity.

Applying the basic viscosity formula, the hinge torque is also given by

$$\tau = \frac{(2\pi r \ell)(r\dot{\phi})}{d} \eta r$$

where r is the mean radius of the inner and outer cylinders, ℓ is the length of the shorter cylinder, and d is the separation between them. (The final r here would better be $(r + d/2)$; however, since d is about 0.004 inch and r is about 0.350 inch, the approximation is very good.) Since the nutation damper design formulas specify k and the cylinder dimensions, the desired viscosity determined from these relations is

$$\eta = \frac{d}{2\pi r^3 \ell} k$$

Note that the units in this formula are centimeter-gram-second (cgs metric); in particular, the lengths are in centimeters and k in dyne-centimeter-second per radian, which will give η in poise. For lengths in inches and k in pound-inch-second per radian, the factor 2.87×10^6 should be used to get η in poise.

During the preparation of the silicone fluid for the hinges, it was found that falling sphere measurement of viscosity was particularly quick and convenient (but usable only with clear fluids). However, a large correction to the basic Stokes' formula was necessary to correct for container size. To make the measurement, a small steel ball-bearing (0.047-inch in diameter) was dropped through the fluid in a cylindrical vial having an inside diameter of about 0.80 inch. The times for the ball to traverse two successive distances were noted. If the velocities thereby obtained were nearly the same, terminal velocity was assumed, at least for the second interval. Repeated drops were made to obtain a good mean. The following formula was then used to find the viscosity:

$$\eta = \frac{2a^2(d_1 - d_2)g}{9V}\left[1 - 2.104\frac{a}{R} + 2.09\left(\frac{a}{R}\right)^3 - 0.95\left(\frac{a}{R}\right)^5 \ldots\right]$$

where

a = radius of the ball

V = terminal velocity of the ball

d_1 = density of the ball

d_2 = density of the fluid

R = inner radius of the cylindrical container

Again the units are centimeter-gram-second metric, yielding η in poises. In this formula, the bracket provides the container (or wall) correction which is known as Faxén's correction. (See, for example, Champion and Davy, "Properties of Matter," Philosophical Library, Inc., page 281.) For the small ball used here, only the first-order correction was made and it was more than 10 percent. Checks made against fluid of reasonably well known viscosity gave confidence in the formula.

Appendix C
TUNING DEPENDENCE ON AMPLITUDE OF NUTATION

In the general theoretical analysis of the motion of the simulator with pendulum dampers, the best dimensions for the arms and their placement are given by

$$\frac{I}{mLa} = \left[\frac{B}{(A - B)}\right]^2$$

or, for a simple pendulum

where

$$I = mL^2$$

its length is

$$L = a\left[\frac{B}{(A-B)}\right]^2$$

This is called the resonance condition. One would expect that this relation could be obtained by looking at the simpler problem of the pendulum swinging in the centrifugal field in the spinning simulator and by saying that the natural frequency should equal the difference between the nutation and spin frequencies similar to the Frahm vibration absorber. This, in fact, had been done before the general analysis was undertaken and there is agreement for small nutation-angles and low-hinge-friction. The results differ, however, by showing the probable effect of larger nutation-angles as well as the usual hinge-friction effect on natural frequency. It is important to note here that whereas the results of the general analysis are only approximate because small angles and angular rates (except spin) are assumed, the following is limited primarily because the nutation angle is assumed to be constant.

In Fig. 31, note that the force exerted by the pendulum bob is

$$F = m\omega_o^2 b$$

where b is measured from the instantaneous center of rotation.

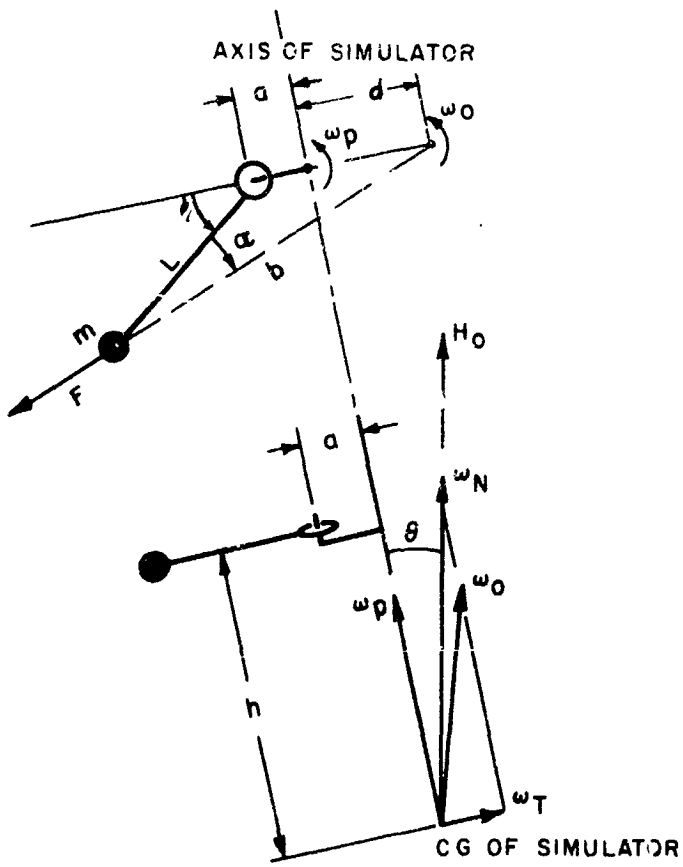

FIG. 31. Centrifugal Field Parameters.

Note that

$$b \sin\alpha = (a + d) \sin\varphi \ .$$

From Fig. 31, note that

$$\frac{d}{h} = \frac{\omega_T}{\omega_p} \ .$$

Also,

$$\omega_T = \omega_N \sin\theta$$

and

$$\frac{\omega_N}{\omega_p} = \frac{A}{B\cos\theta}$$

from which

$$d = h\left(\frac{A}{B}\right)\tan\theta$$

Here ω_o is the total angular velocity vector. It is resolved into two components, ω_p along the symmetry axis of the simulator and ω_T perpendicular to it. The quantity ω_N is the frequency of nutation or the angular velocity at which the axis of the simulator rotates about the total angular momentum vector, H_o, which is fixed in space because there are no outside torques. The amplitude of nutation is the angle θ.

In this simplified concept, the differential equation for the pendulum is then

$$I\ddot{\phi} + k\dot{\phi} + LF\sin\alpha = 0$$

or

$$I\ddot{\phi} + k\dot{\phi} + Lm\omega_o^2\left[a + h\left(\frac{A}{B}\right)\tan\theta\right]\sin\phi = 0$$

where

I = moment of inertia of the pendulum about its hinge

k = hinge-friction coefficient

A = polar moment of inertia of the simulator

B = transverse moment of inertia of the simulator

Other quantities are shown in the figure.

The solution shows that for ϕ not too large, the natural frequency (radians per second) is

$$\omega_\beta = \omega_o \sqrt{\frac{mL}{I}\left(a + \frac{hA}{B}\tan\theta\right) - \left(\frac{k}{2I\omega_o}\right)^2}$$

For a vibration absorber this should match

$$\omega_N - \omega_p \doteq \left(\frac{A}{B} - 1\right)\omega_o$$

or

$$\left(\frac{A}{B} - 1\right)^2 = \frac{mL}{I}\left(a + h\left(\frac{A}{B}\right)\tan\theta\right) - \left(\frac{k}{2I\omega_o}\right)^2$$

If the hinge-friction term is neglected, and if we let

$$I = mL^2,$$

then

$$L = \frac{a + h\left(\frac{A}{B}\right)\tan\theta}{\left(\frac{A}{B} - 1\right)^2}$$

as given in the body of the report.

The value of hinge-friction coefficient, which should give critical damping, is found here also

$$k_c = 2\omega_o \sqrt{mLI\left[a + h\left(\frac{A}{B}\right)\tan\theta\right]}$$

This is, of course, dependent on spin which creates the force field.

REFERENCES

1. den Hartog, J. P. Mechanical Vibrations, 4th ed. New York, McGraw-Hill, 1956. P. 93.

2. U. S. Naval Ordnance Test Station. Passive Damping of Wobbling Satellites. Part 1. General Stability Theory and First Example, by William R. Haseltine. China Lake, Calif., NOTS, 31 July 1959. (NAVORD Report 6579, Part 1, NOTS TP 2306), pp. 14.

3. Newkirk, H. L., W. R. Haseltine, and A. V. Pratt. "Stability of Rotating Space Vehicles," INST RADIO ENGR, PROC, Vol. 48, No. 4 (April 1960), pp. 743-750

4. Haseltine, W. R. "Nutation Damping Rates for a Spinning Satellite," AERO SPACE ENGR, Vol. 21, No. 3 (March 1962), pp. 10-17.